

# Solutions to the Exercises

in A Breviary of Seismic Tomography

Yue Tian and Guust Nolet





# Contents

<b>1</b>	<b>Preface</b>	<i>page 5</i>
<b>2</b>	<b>Ray theory for seismic waves</b>	6
<b>3</b>	<b>Ray tracing</b>	14
<b>4</b>	<b>Wave scattering</b>	22
<b>5</b>	<b>Amplitudes of body waves</b>	30
<b>6</b>	<b>Travel times: observations</b>	34
<b>7</b>	<b>Travel times: interpretation</b>	36
<b>8</b>	<b>Body wave amplitudes: Observation and interpretation</b>	41
<b>9</b>	<b>Normal modes</b>	43
<b>10</b>	<b>Surface wave interpretation: ray theory</b>	47
<b>11</b>	<b>Surface waves: Finite frequency theory</b>	50
<b>12</b>	<b>Model parametrization</b>	53
<b>13</b>	<b>Common corrections</b>	58
<b>14</b>	<b>Linear inversion</b>	60
<b>15</b>	<b>Resolution and error analysis</b>	62
<b>16</b>	<b>Anisotropy</b>	63

# 1

## Preface

Solving exercises is essential to master a subject as complicated as seismic tomography: it transforms the passive activity of reading the textbook into an active learning process, provides feedback and deepens the understanding.

Ideally, exercises are designed such that they are solvable using the knowledge gained, with more or less effort depending on the ability of the student. However, even a strong student may wish to check whether his solution is correct, whereas a weaker student may at times give up on a difficult problem. For that reason we provide elaborate solutions to the exercises in *A Breviary of Seismic Tomography*.

The numbering of the following chapters is identical to the numbering used in *Breviary*.

## 2

### Ray theory for seismic waves

**Exercise 2.1** See Fig. B2.2†, let the angle of rotation be  $\alpha$ . The change of  $u_x$  along  $y$ -direction is

$$\Delta u_x = u_x(x, y + dy) - u_x(x, y) = -dy \sin \alpha - 0 = -dy \sin \alpha.$$

The change of  $u_y$  along  $x$ -direction is

$$\Delta u_y = u_y(x + dx, y) - u_y(x, y) = dx \sin \alpha - 0 = dx \sin \alpha.$$

Thus

$$\frac{\partial u_x}{\partial y} = \lim_{dy \rightarrow 0} \frac{\Delta u_x}{dy} = -\sin \alpha, \quad (2.1)$$

$$\frac{\partial u_y}{\partial x} = \lim_{dx \rightarrow 0} \frac{\Delta u_y}{dx} = \sin \alpha. \quad (2.2)$$

Adding (2.1) and (2.2) gives

$$\frac{\partial u_x}{\partial y} + \frac{\partial u_y}{\partial x} = 0.$$

By definition of strain tensor, we have

$$\epsilon_{12} = \epsilon_{xy} = \frac{1}{2} \left( \frac{\partial u_x}{\partial y} + \frac{\partial u_y}{\partial x} \right) = 0.$$

The above proof can be repeated for all permutations of  $i, j = 1, 2, 3$ . Therefore a pure rotation gives rise to  $\epsilon_{ij} \equiv 0$ .

† When numbers for figures or equations are preceded by a B they refer to figures/equations in A Breviary for Seismic Tomography.

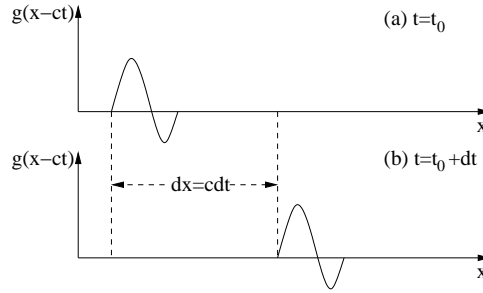


Fig. 2.1. Function  $g(x - ct)$  represents a propagating wave with velocity  $c$  in the  $+x$  direction.

**Exercise 2.2** The inverse Fourier transform gives

$$p(t) = \frac{1}{2\pi} \int_{-\infty}^{\infty} P(\omega) e^{-i\omega t} d\omega.$$

Inserting the condition  $P(\omega) = P(-\omega)^*$ , we get

$$p(t) = \frac{1}{2\pi} \int_{-\infty}^{\infty} P(-\omega)^* e^{-i\omega t} d\omega = -\frac{1}{2\pi} \int_{-\infty}^{\infty} P(-\omega)^* e^{-i\omega t} d(-\omega).$$

Let  $w = -\omega$ , then

$$p(t) = \frac{1}{2\pi} \int_{-\infty}^{\infty} P(w)^* e^{i\omega t} dw = p(t)^*.$$

Hence  $p(t)$  is real.

**Exercise 2.3** Applying the chain rule of differentiation to any differentiable function of the form  $g(x - ct)$  yields

$$\begin{aligned} \frac{\partial P}{\partial t} &= -cg', & \frac{\partial^2 P}{\partial t^2} &= c^2 g'', \\ \frac{\partial P}{\partial x} &= g', & \frac{\partial^2 P}{\partial x^2} &= g'', \end{aligned} \quad (2.3)$$

where  $g'$  and  $g''$  are the first and second order derivatives with respect to the argument  $x - ct$ . Inserting (2.3) into (B2.19) we get  $c^2 g'' \equiv c^2 g''$ .

To see that the solution describes propagating waves, imagine that at  $t = t_0$ ,  $g(x - ct)$  represents a wave as shown in Figure 2.1a. At  $t = t_0 + dt$ , the argument  $x - ct$  will remain unchanged if the distance  $x$  increases by  $dx = cdt$ , and thus the shape of function  $g(x - ct)$  will remain the same (Figure 2.1b). Therefore,  $g(x - ct)$  describes a wave propagating with velocity  $dx/dt = c$  in the  $+x$  direction.

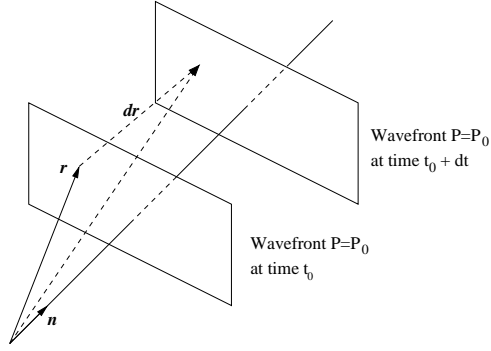


Fig. 2.2. Equation (2.4) describes a plane wave propagating with velocity  $c$  in the direction of  $\hat{\mathbf{n}}$ .

**Exercise 2.4** Applying the chain rule of differentiation to any differentiable function of the form

$$P(x, y, z, t) = g(n_x x + n_y y + n_z z - ct) = g(\hat{\mathbf{n}} \cdot \mathbf{r} - ct) \quad (2.4)$$

yields

$$\begin{aligned} \frac{\partial P}{\partial t} &= -cg', & \frac{\partial^2 P}{\partial t^2} &= c^2 g'', \\ \frac{\partial P}{\partial x} &= n_x g', & \frac{\partial^2 P}{\partial x^2} &= n_x^2 g'', \\ \frac{\partial P}{\partial y} &= n_y g', & \frac{\partial^2 P}{\partial y^2} &= n_y^2 g'', \\ \frac{\partial P}{\partial z} &= n_z g', & \frac{\partial^2 P}{\partial z^2} &= n_z^2 g'', \end{aligned} \quad (2.5)$$

where  $g'$  and  $g''$  are the first and second order derivatives with respect to the argument  $\hat{\mathbf{n}} \cdot \mathbf{r} - ct$ . Inserting (2.5) into the 3-D wave equation (B2.12) without a force (such that it is a propagating wave), we obtain

$$c^2(n_x^2 + n_y^2 + n_z^2)g'' = c^2 g''.$$

Since  $n_x^2 + n_y^2 + n_z^2 = 1$  ( $\hat{\mathbf{n}}$  is a unit vector), the above equation is always true. Thus, (2.4) always satisfies the 3-D wave equation (B2.12).

A wavefront is a surface of constant pressure ( $P = P_0$  in Figure 2.2). A constant argument of function  $g$

$$\hat{\mathbf{n}} \cdot \mathbf{r} - ct = \text{constant} \quad (2.6)$$

therefore guarantees constant  $P$ . At time  $t = t_0$ , (2.6) represents a plane with its normal vector being  $\hat{\mathbf{n}}$ , because all the points in this plane have the same value of  $\hat{\mathbf{n}} \cdot \mathbf{r}$  (Figure 2.2). At time  $t = t_0 + dt$ , (2.6) remains the same constant if the position change  $d\mathbf{r}$  satisfies  $d\mathbf{r} \cdot \hat{\mathbf{n}} = cdt$ , and the simplest case is  $d\mathbf{r} = cdt\hat{\mathbf{n}}$ . Therefore, (2.4) describes a plane wave propagating with velocity  $d\mathbf{r}/dt = c$  in the direction of  $\hat{\mathbf{n}}$ . (It can also propagate in other directions represented by  $d\mathbf{r}$  so long as  $d\mathbf{r} \cdot \hat{\mathbf{n}} = cdt$  is satisfied.)

**Exercise 2.5** Applying the chain rule of differentiation to any differentiable function of the form  $P(r, t) = \frac{1}{r}g(t - r/c)$  yields

$$\begin{aligned}\frac{\partial P}{\partial r} &= -\frac{1}{r^2}g + \frac{1}{r}\left(-\frac{1}{c}\right)g' = -\frac{1}{r^2}g - \frac{1}{cr}g', \\ \frac{\partial^2 P}{\partial r^2} &= \frac{2}{r^3}g - \frac{1}{r^2}\left(-\frac{1}{c}\right)g' - \frac{1}{c}\left(-\frac{1}{r^2}\right)g' - \frac{1}{cr}\left(-\frac{1}{c}\right)g'' = \frac{2}{r^3}g + \frac{2}{cr^2}g' + \frac{1}{c^2r}g'', \\ \frac{\partial P}{\partial t} &= \frac{1}{r}g', \quad \frac{\partial^2 P}{\partial t^2} = \frac{1}{r}g'',\end{aligned}\tag{2.7}$$

where  $g'$  and  $g''$  are the first and second order derivatives with respect to the argument  $t - r/c$ . Inserting (2.7) into (B2.18), we obtain

$$\nabla^2 P = \frac{2}{r^3}g + \frac{2}{cr^2}g' + \frac{1}{c^2r}g'' + \frac{2}{r}\left(-\frac{1}{r^2}g - \frac{1}{cr}g'\right) = \frac{1}{c^2r}g'' = \frac{1}{c^2}\frac{\partial^2 P}{\partial t^2}.$$

This describes a spherical wave. Its wavefront is a sphere centred at  $\mathbf{r} = 0$  and expanding with velocity  $d\mathbf{r}/dt = c$ . Energy on the wavefront must be conserved. Since the energy per unit area is proportional to  $|P|^2$ , and the area of the wavefront is  $4\pi r^2$ , conservation of energy requires  $|P|^2 \cdot 4\pi r^2$  to be constant. Hence we must have  $|P| \propto 1/r$ , i.e. the pressure amplitude  $|P|$  has to diminish as  $1/r$  to conserve energy.

For a wave in a two-dimensional membrane, the wave front is a circle and its perimeter is  $2\pi r$ . Conservation of energy requires  $|P|^2 \cdot 2\pi r$  to be constant, so the amplitude  $|P|$  diminishes as  $1/\sqrt{r}$ .

**Exercise 2.6** The definition of the slowness vector  $\mathbf{p}$  is

$$\mathbf{p} = \frac{1}{c} \frac{d\mathbf{r}}{ds},\tag{2.8}$$

where  $d\mathbf{r}$  is a tangent vector of length  $ds$  along the ray. Since  $d\mathbf{r} = (dx, dy, dz)$ , (2.8) becomes

$$\mathbf{p} = \frac{1}{c} \left( \frac{dx}{ds}, \frac{dy}{ds}, \frac{dz}{ds} \right) = \frac{1}{c} (\gamma_1, \gamma_2, \gamma_3),\tag{2.9}$$

i.e., the elements of  $\mathbf{p}$  are equal to the direction cosines of the ray path scaled by  $1/c$ . Equation (2.9) gives the physical meaning of the slowness vector  $\mathbf{p}$ : its direction is the ray path direction, and its magnitude is equal to the slowness.

**Exercise 2.7** By definition, the magnitude of the cross product is

$$|\mathbf{r} \times \mathbf{p}| = |\mathbf{r}||\mathbf{p}| \sin \langle \mathbf{r}, \mathbf{p} \rangle \quad (2.10)$$

where  $\langle \mathbf{r}, \mathbf{p} \rangle$  represents the angle between  $\mathbf{r}$  and  $\mathbf{p}$ . In a spherical earth, this is the incidence angle  $i$ . We also have  $|\mathbf{r}| = r$  and  $|\mathbf{p}| = 1/c$  (see 2.9), so that (2.10) becomes

$$|\mathbf{r} \times \mathbf{p}| = r \sin i/c.$$

**Exercise 2.8** The spherical slowness is defined in (B2.33) as

$$p = \frac{r \sin i}{c}.$$

At first sight, therefore, it would seem that the unit for the spherical slowness is

$$[p] = \frac{\text{m}}{\text{m/s}} = \text{s},$$

which is a unit of time, not slowness (inverse velocity)! However, we are analysing a wave that travels over an angle and when angles are involved, one should always check if the result depends on the unit of the angle – if so this forces us to specify the angle in its SI unit, the radian<sup>†</sup>. Angles are ‘fractions’ of a circle, inherently dimensionless, and they do not always show up in a dimension analysis as we just did. A look at (B2.32) shows that  $\sin i$  originated from the ratio between  $r d\phi$  and  $ds$ , where  $r d\phi$  has unit of length and here  $r$  must therefore be expressed in m/rad, forcing (B2.33) to give  $p$  explicitly in s/rad. A different and more direct approach uses  $p = dT/d\Delta$ , to give the same result:

$$[p] = \frac{\text{s}}{\text{rad}},$$

and upon reflection this must be the correct unit, since a propagation over an angle is added that provides the missing unit to make it a slowness.

For an earth with surface radius  $r = 6371$  km,  $673$  s/rad corresponds to a surface distance of  $r\Delta = r/p = 6371/673 \approx 10$  km travelled in one second. Thus, the ray’s apparent surface velocity is  $10$  km/s.

<sup>†</sup> A good discussion of this principle can be found in G.J. Aubrecht et al., The Radian – That Troublesome Unit, *The Physics Teacher*, **31**, 84-87, 1993: the radian is a ‘supplementary’ unit in the *Système International d’Unités* (SI). When SI units are consistently used in a formula, no conversion factors are needed to obtain the correct numerical values. For example when we write  $\sin i \approx i$  for small  $i$ , we express  $i$  in radians. Degree is not an SI unit; if we decide to express  $\Delta$  in degrees, we could express  $p$  in s/deg, but (B2.33) would then need a conversion factor if this *numerical* value of  $p$  is used in it to find  $i$ .

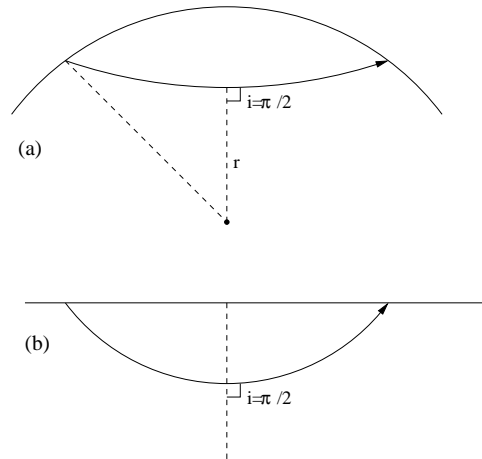


Fig. 2.3. The ray's bottoming point ( $i = \pi/2$ ) in: (a) a spherically symmetric earth; (b) a horizontally layered medium.

**Exercise 2.9** In a spherically symmetric earth,  $p = r \sin i/c$ . The special case  $p = r/c$  occurs when the incidence angle  $i = \pi/2$ . This is the point where the ray bottoms, and the ray path is perpendicular to the vertical direction (Figure 2.3a).

Note: in a horizontally layered medium (Figure 2.3b), the ray also bottoms at the point of  $i = \pi/2$ . The horizontal slowness at the bottoming point is  $p_x = \sin(\pi/2)/c = 1/c$ .

**Exercise 2.10** From (B2.35) and the chain rule of differentiation, we have

$$\begin{aligned} \frac{d\phi}{dr} &= \left( \frac{dr}{d\phi} \right)^{-1} = \frac{1}{r \cot i} = \frac{\tan i}{r}, \\ \frac{di}{dr} &= \frac{di}{d\phi} \frac{d\phi}{dr} = \left( \frac{dc}{dr} \frac{r}{c} - 1 \right) \frac{\tan i}{r} = \tan i \left( \frac{dc}{c dr} - \frac{1}{r} \right). \end{aligned} \quad (2.11)$$

**Exercise 2.11** From (B2.32)

$$dT = \frac{ds}{c} = \frac{dr}{c \cos i}. \quad (2.12)$$

From (B2.33)

$$\sin i = pc/r,$$

$$\cos i = \sqrt{1 - \sin^2 i} = \sqrt{1 - p^2 c^2 / r^2}. \quad (2.13)$$

Inserting (2.13) into (2.12)

$$dT = \frac{dr}{c\sqrt{1 - p^2c^2/r^2}},$$

and hence

$$T(p) = \int dT = \int \frac{dr}{c\sqrt{1 - p^2c^2/r^2}}. \quad (2.14)$$

From (2.13)

$$\tan i = \frac{\sin i}{\cos i} = \frac{pc/r}{\sqrt{1 - p^2c^2/r^2}} = \frac{1}{\sqrt{r^2/p^2c^2 - 1}}. \quad (2.15)$$

From (2.11),  $d\phi = \tan i \, dr/r$ . Inserting (2.15), we get

$$d\phi = \tan i \, dr/r = \frac{dr}{r\sqrt{r^2/p^2c^2 - 1}}.$$

Epical distance  $\Delta$  is the integral of  $d\phi$ :

$$\Delta(p) = \int d\phi = \int \frac{dr}{r\sqrt{r^2/p^2c^2 - 1}}. \quad (2.16)$$

**Exercise 2.12** For a ray from an earthquake at depth  $h$  to a surface station, the travel time in (2.14) can be expressed as a sum of two integrals: one is from the bottoming point to the earthquake at a radius  $r = a - h$ ; the other is from the bottoming point to the earth's surface. Therefore

$$T(p) = \int_b^{a-h} \frac{dr}{c\sqrt{1 - p^2c^2/r^2}} + \int_b^a \frac{dr}{c\sqrt{1 - p^2c^2/r^2}}.$$

**Exercise 2.13** According to (B2.44), the direction of displacement of seismic waves is the direction of the amplitude vector  $\mathbf{A}$ . On the other hand,  $\tau(\mathbf{r}) = \text{constant}$  defines the wavefront, so its gradient  $\nabla\tau$  defines the ray direction (perpendicular to the wavefront surface). Equation (B2.46) implies that  $\mathbf{A}$  is perpendicular to  $\nabla\tau$  for S waves, so the direction of displacement of a S wave is perpendicular to the ray direction. From (B2.46) the S wave velocity is  $V_s = \sqrt{\mu/\rho}$ , independent of its polarization (the direction of  $\mathbf{A}$ ).

**Exercise 2.14** Since  $\tau(\mathbf{r}) = \text{constant}$  defines the wavefront, its gradient  $\nabla\tau$  defines the ray direction. (B2.45) says that  $\mathbf{A}$  is parallel to  $\nabla\tau$  for P waves, so the direction of displacement of a P wave is parallel to the ray direction. There is therefore only one polarization direction for P waves: the ray direction.

**Exercise 2.15** In a non-viscous fluid, (B2.45) and (B2.46) become:

$$V_p = \sqrt{\lambda/\rho}, \quad V_s = 0.$$

The acoustic wave velocity is  $c = \sqrt{\kappa/\rho}$  (B2.13) where the bulk modulus  $\kappa \equiv \lambda + \frac{2}{3}\mu$ . For fluids,  $\mu = 0$ , so  $\kappa = \lambda$ , and the acoustic velocity becomes

$$c = \sqrt{\kappa/\rho} = \sqrt{\lambda/\rho} = V_p.$$

Therefore, acoustic waves are P waves in a non-viscous fluid, and there is no S wave in a non-viscous fluid ( $V_s = 0$ ).

**Exercise 2.16** The elastic wave equation in an isotropic, homogeneous earth is

$$\rho \frac{\partial^2 u_i}{\partial t^2} = \sum_j (\lambda + \mu) \frac{\partial^2 u_j}{\partial x_i \partial x_j} + \sum_j \mu \frac{\partial^2 u_i}{\partial x_j^2}. \quad (2.17)$$

We use (B2.10) to define the relationship between displacement and pressure, and applying this to the first term on the r.h.s. of (2.17) yields

$$\rho \frac{\partial^2 u_i}{\partial t^2} = (\lambda + \mu) \frac{\partial}{\partial x_i} \left( -\frac{P}{\kappa} \right) + \sum_j \mu \frac{\partial^2 u_i}{\partial x_j^2}. \quad (2.18)$$

Taking the divergence of (2.18) and again using (B2.10), we get

$$\rho \frac{\partial^2}{\partial t^2} \left( -\frac{P}{\kappa} \right) = \sum_i (\lambda + \mu) \frac{\partial^2}{\partial x_i^2} \left( -\frac{P}{\kappa} \right) + \sum_j \mu \frac{\partial^2}{\partial x_j^2} \left( -\frac{P}{\kappa} \right). \quad (2.19)$$

Multiplying (2.19) by  $-\kappa$  (constant for a homogeneous earth) and merging the two terms on the right

$$\rho \frac{\partial^2 P}{\partial t^2} = \sum_i (\lambda + 2\mu) \frac{\partial^2 P}{\partial x_i^2} = (\lambda + 2\mu) \nabla^2 P. \quad (2.20)$$

Rewriting (2.20) as

$$\frac{\partial^2 P}{\partial t^2} = c^2 \nabla^2 P, \quad (2.21)$$

where  $c = \sqrt{(\lambda + 2\mu)/\rho}$ . (2.21) is a 1-D wave equation in homogeneous media with velocity  $c$ . Thus, pressure  $P$  satisfies the wave equation and propagates with the P wave velocity:  $c = \sqrt{(\lambda + 2\mu)/\rho} = V_p$ .

**Exercise 2.17** Consider a plane wave. Since a cube is flattened by the passage of a P wave, it does not maintain its shape. Nor does a spherical shell in the case of a spherical wave (it is thinned or thickened).

### 3

## Ray tracing

**Exercise 3.1** Figure 3.1 shows the graph with letter for each node. Following the shortest path algorithm gives the following steps:

- (i) Set  $\mathcal{Q} = \{A(T_A = 0), B, C, D(T_B = T_C = T_D = \infty)\}$ . Set  $\mathcal{P}$  is empty.
- (ii) Choose node  $s = A$ , since  $T_A$  is the smallest in set  $\mathcal{Q}$ . The forward star of node  $A$  in set  $\mathcal{Q}$  includes nodes  $B$  and  $D$ . Update the travel times and ray paths for nodes  $B$  and  $D$ :  $T_B = \min\{T_B, T_A + \Delta T_{AB}\} = \min\{\infty, 0 + 3\} = 3$ , ray path  $AB$ ;  $T_D = \min\{T_D, T_A + \Delta T_{AD}\} = \min\{\infty, 0 + 1\} = 1$ , ray path  $AD$ . Move node  $A$  from set  $\mathcal{Q}$  to set  $\mathcal{P}$ . Now set  $\mathcal{Q} = \{B(T_B = 3, \text{ray path } AB); C(T_C = \infty); D(T_D = 1, \text{ray path } AD)\}$ , set  $\mathcal{P} = \{A(T_A = 0)\}$ .
- (iii) Choose node  $s = D$ , since  $T_D$  is the smallest in set  $\mathcal{Q}$ . The forward star of node  $D$  in set  $\mathcal{Q}$  includes nodes  $B$  and  $C$ . Update the travel times and ray paths for nodes  $B$  and  $C$ :  $T_B = \min\{T_B, T_D + \Delta T_{DB}\} =$

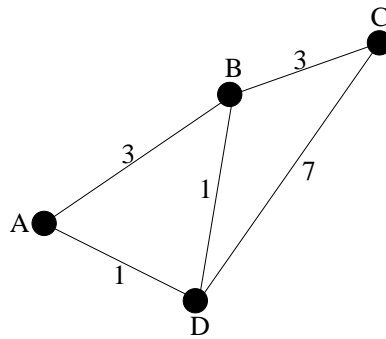


Fig. 3.1. Simple graph for the shortest path method.

```

subroutine shpath(is,tt,prec,h,q,np)

dimension tt(np),prec (np),h(np),q(np)
dimension fs(1000),fsd(1000)
integer prec ,h,q,fs,fsv,u,v
data rinf/1.0e30/

do i=1,np          ! put all nodes in set Q
  prec(i)=is
  tt(i)=rinf
  h(i)=-1
  q(i)=-1
end do
tt(is)=0.0        ! step (i)
q(1)=is           ! move source into the heap (set Q with t<inf)
h(is)=1
iq=1
do while (iq.gt.0)      ! step (ii)
  u=q(1)           ! step (v)
  h(q(iq))=1
  h(u)=-1
  q(1)=q(iq)
  q(iq)=-1
  iq=iq-1
  k=1
  call cheap(iq,k,tt,h,q,np)      ! step (iii)
  call forstar(u,np,fs,fsd,nf)
  do v=1,nf
    fsv=fs(v)
    z=fsd(v)+tt(u)
    if (z.lt.tt(fsv)) then
      tt(fsv)=z                    ! step (iv)
      prec(fsv)=u
      k=h(fsv)
      if (k.le.0) then
        iq=iq+1
        k=iq
        h(fsv)=iq
        q(iq)=fsv
      endif
      call cheap(iq,k,tt,h,q,np) ! step (iii)
    endif
  enddo
enddo
return
end

```

Fig. 3.2. Subroutine shpath with steps identified.

$\min\{3, 1 + 1\} = 2$ , ray path  $ADB$ ;  $T_C = \min\{T_C, T_D + \Delta T_{DC}\} =$   
 $\min\{\infty, 1 + 7\} = 8$ , ray path  $ADC$ . Move node  $D$  from set  $Q$  to set  $\mathcal{P}$ .  
 Now set  $Q = \{B (T_B = 2, \text{ray path } ADB); C (T_C = 8, \text{ray path } ADC)\}$ ,  
 set  $\mathcal{P} = \{A (T_A = 0); D (T_D = 1, \text{ray path } AD)\}$ .

- (iv) Choose node  $s = B$ , since  $T_B$  is the smallest in set  $Q$ . The forward star of node  $B$  in set  $Q$  includes node  $C$ . Update the travel time and ray

```

program tstsp
! test shpath on 10*10 'Streets of New York' model
! output:
! 'tt.xy': time plot file for GMT
! 'ray.xy': ray plot file for GMT
dimension tt(100)
integer prec(100),h(100),q(100)
np=100
is=55          ! source at center
call shpath(is,tt,prec,h,q,np)
n=0
open(1,file='tt.xy')    ! time plot file for GMT
open(2,file='ray.xy')  ! ray plot file for GMT
do j=1,10              ! j=y coordinate
  do i=1,10            ! i=x coordinate
    n=n+1              ! index of node (i,j)
    write(1,*) i,j,tt(n)
    write(2,*) i,j
    jprec=(prec(n)-1)/10+1 ! j of preceding ray node
    iprec=prec(n)-10*(jprec-1) ! i of preceding ray node
    write(2,*) iprec,jprec
    write(2,fmt='(a)') '>'
  enddo
enddo
close(1)
close(2)
end

```

Fig. 3.3. Fortran program that calls subroutine `shpath` for a  $10 \times 10$  2-D homogeneous model with a source at node (5, 6).

path for node  $C$ :  $T_C = \min\{T_C, T_B + \Delta T_{BC}\} = \min\{8, 2 + 3\} = 5$ , ray path  $ADBC$ . Move node  $B$  from set  $\mathcal{Q}$  to set  $\mathcal{P}$ . Now set  $\mathcal{Q} = \{C (T_C = 5, \text{ray path } ADBC)\}$ , set  $\mathcal{P} = \{A (T_A = 0); B (T_B = 2, \text{ray path } ADB); D (T_D = 1, \text{ray path } AD)\}$ .

- (v) Choose node  $s = C$ , since  $T_C$  is the smallest (the only node) in set  $\mathcal{Q}$ . There is no forward star of node  $C$  and no travel time to update. Move node  $C$  from set  $\mathcal{Q}$  to set  $\mathcal{P}$ . Now set  $\mathcal{Q}$  is empty, set  $\mathcal{P} = \{A (T_A = 0); B (T_B = 2, \text{ray path } ADB); C (T_C = 5, \text{ray path } ADBC); D (T_D = 1, \text{ray path } AD)\}$ .
- (vi) Since set  $\mathcal{Q}$  is empty, stop. The final set  $\mathcal{P}$  gives the travel times and ray paths from node  $A$  to the other three nodes.

**Exercise 3.2** In `shpath`, the heap  $h$  contains all  $iq$  nodes with a provisional travel time less than the initial (infinite) time; the top of the heap has the node with the shortest time and is removed from the heap (into set  $\mathcal{P}$ , which is not explicitly identified in `shpath`). The steps are identified in Figure 3.2.

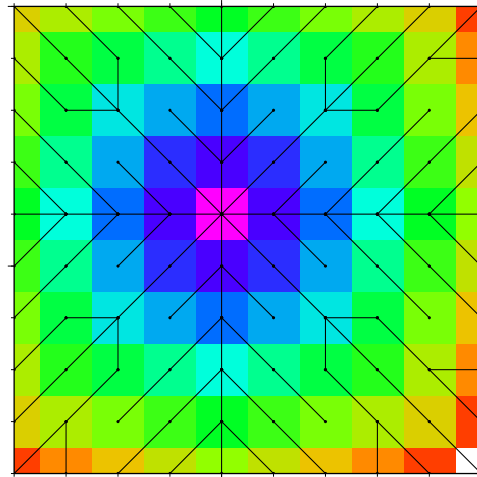


Fig. 3.4. Ray paths from the source node (5, 6) to all other nodes for a  $10 \times 10$  2-D homogeneous model.

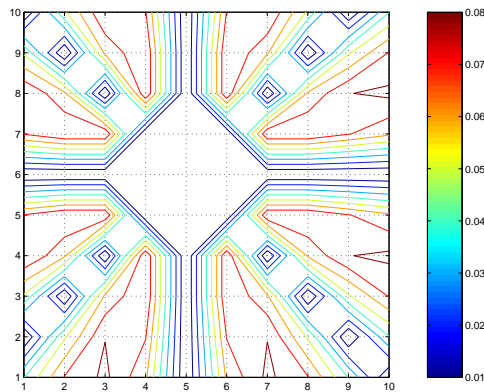


Fig. 3.5. Contour of the relative travel time errors (in percent) for rays in Figure 3.4.

**Exercise 3.3** Figure 3.3 gives the Fortran program that calls subroutine shpath for a  $10 \times 10$  2-D homogeneous model with a source at node (5, 6).

Figure 3.4 shows the ray paths from the source node to all other nodes in this model. The theoretical ray paths are straight lines but this is only correctly computed for nodes in four directions (taking the source node as the origin): N-S, E-W, NW-ES, and NE-SW. For other nodes, the ray paths are longer than the theoretical straight line paths, and so yield longer travel times.

Figure 3.5 shows the contour of the relative travel time errors. Similar to the rays in Figure 3.4, there are 4 directions of zero travel time error: N-S, E-W, NW-ES,

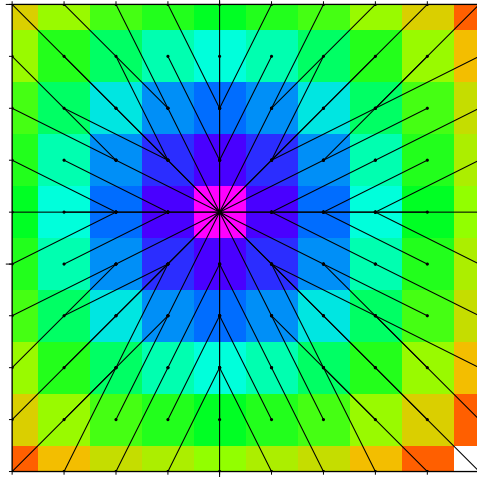


Fig. 3.6. The same as Figure 3.4, except that subroutine `forstar` is extended to include one more row/column on each side of the source node.

and NE-SW. Between these 4 directions, the relative travel time error gradually increases, and the maximum error is reached in the middle between two adjacent zero error directions. The maximum relative error is about 8%.

**Exercise 3.4** To extend the `forstar` subroutine to include one more row/column on each side of the source node, we only need to change lines 14-15 in subroutine `forstar` to:

```
do jj = max(1, j-1), min(n, j+1)
  do ii = max(1, i-1), min(n, i+1)
```

Figure 3.6 shows the ray paths from the source node to all other nodes in this model. Compared with the rays in Figure 3.4 (computed with a smaller forward star), there are more straight line paths and there are more than one shortest path to some nodes in Figure 3.6.

Figure 3.7 shows the contour of the relative travel time errors. Again we take the source node (5,6) as the origin and compare it with Figure 3.5. It is clear that the overall error level drops because the forward star now includes more nodes and thus provides shorter paths, with the maximum relative error of only 2.5%. There are also more zero error nodes. Besides the 4 directions of zero error (N-S, E-W, NW-ES, NE-SW), the zero error region in the centre expands to the larger forward star of the origin, and there are 8 more zero error nodes at the corners (e.g. nodes (2,3)

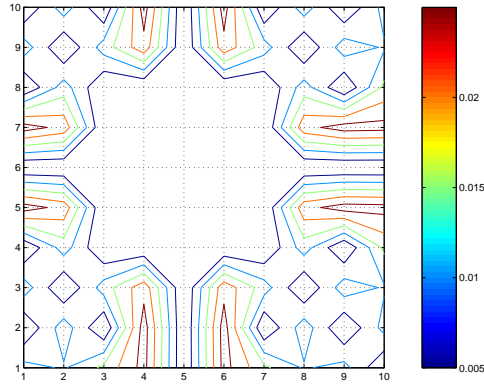


Fig. 3.7. The same as Figure 3.5, except that subroutine `forstar` is extended to include one more row/column on each side of the source node.

and (2,7)). The maximum error region moves towards the N-S and E-W directions.

**Exercise 3.5** For a velocity increasing linearly with column number  $i$  :  $v(i) = 1 + (i - 1)/9$ , the adapted `forstar` subroutine is shown in Figure 3.8.

Figure 3.9 shows the ray paths from the source node to all other nodes in this model. It's different from Figure 3.6 in that there is only one shortest time path for each node, because the velocity is no longer homogeneous. Also the ray path is no longer symmetric about  $i = 5$  because the velocity is no longer symmetric about  $i = 5$ . The rays do not represent the reflection or transmission behaviour when they encounter a velocity boundary, which suggests that the shortest path method is not very accurate.

```

subroutine forstar(u,np,fs,fsd,nf)

! example for square 2-D medium with node spacing 1
! velocity increases linearly with i (column number)
! from v=1 at i=1 to v=2 at i=10
! input: node u, dimension n=sqrt(np)
! output: fsd(i) is the travel time between u and fs(i), i=1,...,nf

dimension fs(1000),fsd(1000)
integer u,fs

n=sqrt(0.001+np)
j=(u-1)/n+1 ! row number of node u in the square grid
i=u-n*(j-1) ! column number
vu = 1. + (i-1.)/9. ! velocity at node u
nf=0
do jj=max(1,j-2),min(n,j+2)
  do ii=max(1,i-2),min(n,i+2)
    ds=sqrt(0.+(ii-i)**2+(jj-j)**2) ! distance (ii,jj) to u
    if(ds.gt.0.) then
      vii = 1. + (ii-1.)/9.
      velocity=(vu+vii)/2. ! average velocity between (ii,jj) and u
      nf=nf+1
      if(nf.gt.1000) stop 'dimension of fs exceeded'
      fs(nf)=(jj-1)*n+ii ! sequential index of node (ii,jj)
      fsd(nf)=ds/velocity
    endif
  enddo
enddo
return
end

```

Fig. 3.8. Adapted forstar subroutine for a velocity increasing linearly with the column number.

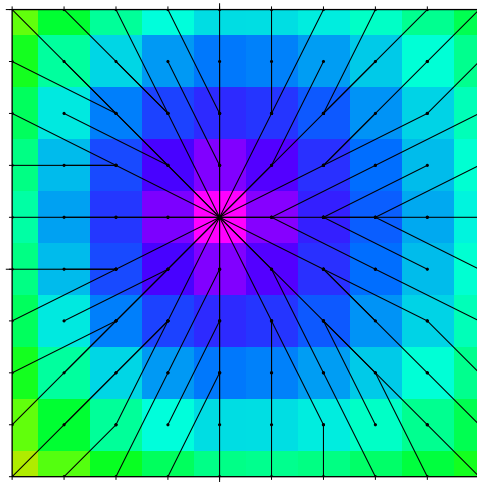


Fig. 3.9. Ray paths for a velocity increasing linearly with column number. The source is at node (5, 6). The forward star is the same as in Exercise 3.4.

**Exercise 3.6** To simplify expressions, we use  $f = \sqrt{1 - c^2(p_1^2 + p_2^2)}$ , noting that  $f = 1$  and  $\partial_i f = 0$  on the ray where  $p_1 = p_2 = 0$ .

(a)  $\partial_i \mathcal{H} = -\partial_i(\partial\tau/\partial s) = -\partial(\partial_i\tau)/\partial s = 0$ , since  $\partial_i\tau = 0$  independent of  $s$  along the ray. Therefore  $-\partial_1\mathcal{H} = \partial_1(hf/c) = \partial_1(h/c)f = 0$  or  $\partial_1(h/c) = 0$ .

(b)  $h = 1 - Kq_1 = 1$  on the ray where  $q_1 = 0$ .

(c) Differentiating the expression (B3.5) for  $\mathcal{H}$ :

$$\begin{aligned}\partial_i \mathcal{H} &= \frac{(h\partial_i c - c\partial_i h)[1 - c^2(p_1^2 + p_2^2)] + hc^2\partial_i c(p_1^2 + p_2^2)}{c^2 f} \\ &= \frac{h\partial_i c - c\partial_i h[1 - c^2(p_1^2 + p_2^2)]}{c^2 f}.\end{aligned}$$

(d)  $\partial\mathcal{H}/\partial p_i = -\partial(hf/c)/\partial p_i = hcp_i/f$ , which is zero on the ray because  $p_i = 0$ .

(e) Since the first derivatives of  $\mathcal{H}$  are zero, the second-order Taylor expansion is (summing over  $i$  and  $j = 1, 2$  is implied):

$$\mathcal{H} \approx \mathcal{H}(0, 0, 0, 0) + \frac{1}{2} \frac{\partial^2 \mathcal{H}}{\partial q_i^2} q_i^2 + \frac{\partial^2 \mathcal{H}}{\partial q_i \partial p_j} q_i p_j + \frac{1}{2} \frac{\partial^2 \mathcal{H}}{\partial p_i^2} p_i^2.$$

The derivatives in the above equation are on the ray and assumed constant, so that for example  $\partial\mathcal{H}/\partial p_k = (\partial^2\mathcal{H}/\partial p_k \partial q_j)q_j + (\partial^2\mathcal{H}/\partial p_k^2)p_k$ , which is zero on the ray where  $q_i$  and  $p_i$  are zero.

(f) From (c):  $\partial_1\mathcal{H} = (h\partial_1 c - cf^2\partial_1 h)/c^2 f$ . On the ray, where  $f = 1$  and  $\partial_1 f = 0$ :

$$\frac{\partial^2 \mathcal{H}}{\partial q_1^2} = \frac{h\partial_{11}c - c\partial_{11}h}{c^2} - \frac{h\partial_1 c - c\partial_1 h}{c^3} 2\partial_1 c$$

The second term is zero because of the result proven in (a). Since  $h = 1 - Kq_1$ , the second-order derivative  $\partial_{11}h = 0$ . Therefore  $\partial_{11}\mathcal{H} = \partial_{11}c/c^2$ .

**Exercise 3.7** This follows from a first-order Taylor expansion:

$$\tau = \frac{\sqrt{z^2 + x^2 + y^2}}{c} = \frac{z}{c} \sqrt{1 + \frac{x^2 + y^2}{z^2}} \approx \frac{z}{c} \left( 1 + \frac{x^2 + y^2}{2z^2} \right)$$

From this:  $H_{11} = \partial^2\tau/\partial x^2 = 1/zc$ , and  $H_{22} = 1/zc$ . Close to the axis  $z \approx s$ , so  $\mathbf{H} \approx \frac{1}{cs}\mathbf{I}$ .

**Exercise 3.8**  $d\mathbf{P}/ds = (d\mathbf{H}/ds)\mathbf{Q} + \mathbf{H}(d\mathbf{Q}/ds) = (-c^{-1}\mathbf{V} - c\mathbf{H}^2)\mathbf{Q} + c\mathbf{H}^2\mathbf{Q} = -c^{-2}\mathbf{V}$

## 4

### Wave scattering

**Exercise 4.1** From (B2.48) follows that the diameter of Fresnel zone is  $d_{max} = \sqrt{\lambda L}$ . The wavenumber  $k$  equals  $2\pi/\lambda$ . Then

$$D = \frac{4L}{ka^2} = \frac{\lambda}{2\pi} \frac{4L}{a^2} = \frac{2}{\pi} \frac{\lambda L}{a^2} = \frac{2d_{max}^2}{\pi a^2}.$$

**Exercise 4.2** Since scattered waves are *added* to an incoming wavefield that remains unaffected, energy increases in the Born approximation and is not conserved.

**Exercise 4.3** Even though there is no multiple scattering in this case, energy is not conserved so the result is not exact.

**Exercise 4.4** In equation (B4.15), the last two terms on the right hand side represent the far-field response, because the amplitude decreases as  $r^{-1}$ . If the source time function  $\dot{M}_{jk}(t) = \delta(t)$ , then the Fourier transform

$$\int_{-\infty}^{+\infty} \dot{M}_{jk}(t - r/V_P) e^{i\omega t} dt = e^{i\omega r/V_P} = e^{ik_P r},$$

$$\int_{-\infty}^{+\infty} \dot{M}_{jk}(t - r/V_S) e^{i\omega t} dt = e^{i\omega r/V_S} = e^{ik_S r},$$

so that the Fourier spectrum of the far-field response is

$$\partial_k G_i^{jk}(\mathbf{r}, \mathbf{r}', \omega) = \sum_{jk} \left( \frac{\gamma_i \gamma_j \gamma_k}{4\pi \rho V_P^3 r} e^{ik_P r} - \frac{\gamma_i \gamma_j - \delta_{ij}}{4\pi \rho V_S^3 r} \gamma_k e^{ik_S r} \right).$$

If  $\dot{M}$  is a  $\delta$ -function,  $M$  itself is the Heaviside function  $h(t) = \int \delta(t-t')dt'$ , with a spectrum  $i/\omega = -1/i\omega$  (see B2.66), which explains the extra factor  $-i\omega$ .

**Exercise 4.5** In (B4.16), the first term is the dot product of (B4.10) with a force  $\mathbf{f}$ . Since  $\nabla'G$  is the gradient  $\partial G_i^j/\partial x'_k$  we recognize the contraction (B4.13) summed over all moment tensor elements  $M_{jk}$  in the second term.

**Exercise 4.6** Since the far field term contains the time derivative of  $M$ , it is weaker for signals in which the low frequencies are dominant (differentiation in the time domain is equivalent to multiplication with  $-i\omega$  in the frequency domain). In the near field term, the Heaviside function will give a contribution

$$\int_{r/V_P}^{r/V_S} \tau d\tau = \frac{r^2}{2} \left( \frac{1}{V_S^2} - \frac{1}{V_P^2} \right),$$

and displacements only damp as  $r^{-2}$  rather than the  $r^{-4}$  in the denominator of (B4.15). Note also that both the near- and intermediate terms lead to a permanent offset, whereas the far field signal is transient. Whether or not one can ignore the near field terms is therefore dependent on the frequency of interest.

**Exercise 4.7** A unit force in the  $z$ -direction can be expressed with a Kronecker delta as  $f_j(t) = f_z(t)\delta_{j3}$ . Dotting (B4.9) with this gives

$$\begin{aligned} \sum_j G_i^j(\mathbf{r}, t) f_j &= \sum_j \frac{1}{4\pi\rho r^3} (3\gamma_i\gamma_j - \delta_{ij}) \delta_{j3} \int_{r/V_P}^{r/V_S} \tau f_z(t-\tau) d\tau \\ &+ \frac{1}{4\pi\rho V_P^2 r} \gamma_i\gamma_j \delta_{j3} f_z(t-r/V_P) - \frac{1}{4\pi\rho V_S^2 r} (\gamma_i\gamma_j - \delta_{ij}) \delta_{j3} f_z(t-r/V_S) \\ &= \frac{1}{4\pi\rho r^3} (3\gamma_i\gamma_3 - \delta_{i3}) \int_{r/V_P}^{r/V_S} \tau f_z(t-\tau) d\tau \\ &+ \frac{1}{4\pi\rho V_P^2 r} \gamma_i\gamma_3 f_z(t-r/V_P) - \frac{1}{4\pi\rho V_S^2 r} (\gamma_i\gamma_3 - \delta_{i3}) f_z(t-r/V_S). \end{aligned} \quad (4.1)$$

For the component in the  $r$ -direction we must dot (4.1) with the unit vector  $(\gamma_1, \gamma_2, \gamma_3) = (\cos\phi\sin\theta, \sin\phi\sin\theta, \cos\theta)$  in the  $r$ -direction to get

$$\begin{aligned} u_r = \sum_{ij} G_i^j(\mathbf{r}, t) f_j \gamma_i &= \frac{1}{4\pi\rho r^3} (3\gamma_3 - \gamma_3) \int_{r/V_P}^{r/V_S} \tau f_z(t-\tau) d\tau \\ &+ \frac{1}{4\pi\rho V_P^2 r} \gamma_3 f_z(t-r/V_P) - \frac{1}{4\pi\rho V_S^2 r} (\gamma_3 - \gamma_3) f_z(t-r/V_S) \\ &= \frac{\cos\theta}{4\pi\rho r} \left[ \frac{2}{r^2} \int_{r/V_P}^{r/V_S} \tau f_z(t-\tau) d\tau + \frac{1}{V_P^2} f_z(t-r/V_P) \right]. \end{aligned} \quad (4.2)$$

At arbitrary  $\phi$ , the  $\theta$ -direction is given by a vector  $(\cos \phi \cos \theta, \sin \phi \cos \theta, -\sin \theta)$ . We can ease the algebra by recognizing that the expression for  $u_\theta$  must be independent of  $\phi$  because of spherical symmetry. Choosing  $\phi = 0$ , such that  $(\gamma_1, \gamma_2, \gamma_3) = (\sin \theta, 0, \cos \theta)$ . We must dot (4.1) with the unit vector  $(\cos \theta, 0, -\sin \theta)$ :

$$\begin{aligned}
u_r &= \frac{1}{4\pi\rho r^3} (3 \sin \theta \cos^2 \theta - 3 \sin \theta \cos^2 \theta + \sin \theta) \int_{r/V_P}^{r/V_S} \tau f_z(t - \tau) d\tau \\
&+ \frac{1}{4\pi\rho V_P^2 r} (\sin \theta \cos^2 \theta - \sin \theta \cos^2 \theta) f_z(t - r/V_P) \\
&- \frac{1}{4\pi\rho V_S^2 r} (\sin \theta \cos^2 \theta - \sin \theta \cos^2 \theta + \sin \theta) f_z(t - r/V_S) \\
&= \frac{\sin \theta}{4\pi\rho r} \left[ \frac{1}{r^2} \int_{r/V_P}^{r/V_S} \tau f_z(t - \tau) d\tau - \frac{1}{V_S^2} f_z(t - r/V_S) \right]. \tag{4.3}
\end{aligned}$$

For  $f_z(t) = \delta(t)$ :

$$\int_{r/V_P}^{r/V_S} \tau f_z(t - \tau) d\tau = \int_{r/V_P}^{r/V_S} \tau \delta(t - \tau) d\tau = \begin{cases} t & \text{if } r/V_P \leq t \leq r/V_S \\ 0 & \text{otherwise} \end{cases}.$$

Inserting the above equation into (4.2) and (4.3):

$$\begin{aligned}
u_r(\mathbf{r}, t) &= \begin{cases} \frac{\cos \theta}{4\pi\rho r} \left[ \frac{2t}{r^2} + \frac{1}{V_P^2} \delta(t - r/V_P) \right] & \text{if } r/V_P \leq t \leq r/V_S \\ 0 & \text{otherwise} \end{cases}; \\
u_\theta(\mathbf{r}, t) &= \begin{cases} \frac{\sin \theta}{4\pi\rho r} \left[ \frac{t}{r^2} - \frac{1}{V_S^2} \delta(t - r/V_S) \right] & \text{if } r/V_P \leq t \leq r/V_S \\ 0 & \text{otherwise} \end{cases}.
\end{aligned}$$

Figure 4.1 sketches the behaviour of  $u_r$  and  $u_\theta$  with time, with their amplitude decreasing rates denoted.

When  $f_z(t) = H(t)$ :

$$f_z(t - r/V_P) = H(t - r/V_P) = \begin{cases} 1 & \text{if } t \geq r/V_P \\ 0 & \text{if } t < r/V_P \end{cases},$$

$$f_z(t - r/V_S) = H(t - r/V_S) = \begin{cases} 1 & \text{if } t \geq r/V_S \\ 0 & \text{if } t < r/V_S \end{cases},$$

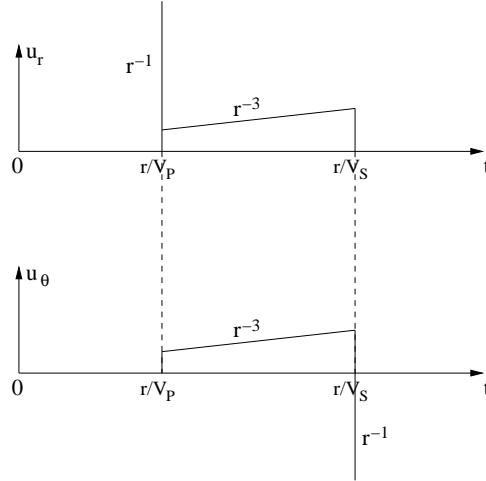


Fig. 4.1. Diagram of  $u_r$  and  $u_\theta$  of a pulse source  $f_z(t) = \delta(t)$ .

$$\begin{aligned} \int_{r/V_P}^{r/V_S} \tau f_z(t - \tau) d\tau &= \int_{r/V_P}^{r/V_S} \tau H(t - \tau) d\tau \\ &= \begin{cases} 0 & \text{if } t < r/V_P \\ \int_{r/V_P}^t \tau d\tau = \frac{1}{2} \left( t^2 - \frac{r^2}{V_P^2} \right) & \text{if } r/V_P \leq t \leq r/V_S \\ \int_{r/V_P}^{r/V_S} \tau d\tau = \frac{r^2}{2} \left( \frac{1}{V_S^2} - \frac{1}{V_P^2} \right) & \text{if } t > r/V_S \end{cases} . \end{aligned}$$

Inserting this into (4.2) and (4.3) gives

$$u_r(\mathbf{r}, t) = \begin{cases} 0 & \text{if } t < r/V_P \\ \frac{t^2 \cos \theta}{4\pi \rho r^3} & \text{if } r/V_P \leq t \leq r/V_S \\ \frac{\cos \theta}{4\pi \rho r V_S^2} & \text{if } t > r/V_S \end{cases} ;$$

$$u_\theta(\mathbf{r}, t) = \begin{cases} 0 & \text{if } t < r/V_P \\ \frac{\sin \theta}{8\pi \rho r^3} \left( t^2 - \frac{r^2}{V_P^2} \right) & \text{if } r/V_P \leq t \leq r/V_S \\ -\frac{\sin \theta}{8\pi \rho r} \left( \frac{1}{V_S^2} + \frac{1}{V_P^2} \right) & \text{if } t > r/V_S \end{cases} .$$

Figure 4.2 sketches the behaviour of  $u_r$  and  $u_\theta$  with time, with their amplitude decreasing rates denoted. The Heaviside function kicks in after  $t = r/V_P$  for  $u_r$  ( $H(t - r/V_P)$ ), which corresponds to far field P waves and again after  $t = r/V_S$  for  $u_\theta$  ( $H(t - r/V_S)$ ), which corresponds to far field S waves. The parabolic behaviour of both  $u_r$  and  $u_\theta$  corresponds to near field waves. It does not have a distinct pulse arrival, but extends between times  $t/V_P$  and  $t/V_S$ , and it cannot be identified with pure P or S waves motion.

## Wave scattering

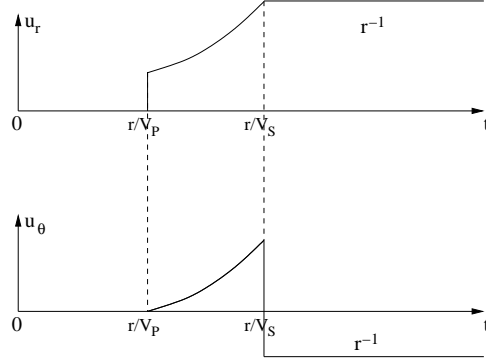


Fig. 4.2. Diagram of  $u_r$  and  $u_\theta$  of a Heaviside source  $f_z(t) = H(t)$ .

**Exercise 4.8** The  $i$ -th element of  $\mathbf{G} \cdot \nabla v$  is

$$\sum_j G_i^j \frac{\partial v}{\partial x_j} = \sum_j \left[ \frac{\partial}{\partial x_j} (v G_i^j) - v \frac{\partial G_i^j}{\partial x_j} \right].$$

Using vector notation the above equation can be written as

$$\mathbf{G} \cdot \nabla v = \nabla \cdot (v \mathbf{G}) - v \nabla \cdot \mathbf{G}.$$

Therefore

$$\int \mathbf{G} \cdot \nabla v \, d^3 \mathbf{r}' = \int \nabla \cdot (v \mathbf{G}) \, d^3 \mathbf{r}' - \int v \nabla \cdot \mathbf{G} \, d^3 \mathbf{r}'.$$

**Exercise 4.9** The component of scattered S wave in the  $\phi$ -direction is (see Figure B4.4)

$$\delta u_\phi^{PS} = -\delta u_x^{PS} \sin \phi + \delta u_y^{PS} \cos \phi. \quad (4.4)$$

The expressions of  $\delta u_i^{PS}$  are

$$\delta u_x^{PS} = \frac{k_s^2 e^{ik_s r}}{4\pi r} \left[ \frac{\delta \rho}{\rho} (\delta_{xz} - \gamma_x \gamma_z) - \frac{2\delta \mu V_s}{\mu V_P} (\delta_{xz} \gamma_z - \gamma_x \gamma_z^2) \right];$$

$$\delta u_y^{PS} = \frac{k_s^2 e^{ik_s r}}{4\pi r} \left[ \frac{\delta \rho}{\rho} (\delta_{yz} - \gamma_y \gamma_z) - \frac{2\delta \mu V_s}{\mu V_P} (\delta_{yz} \gamma_z - \gamma_y \gamma_z^2) \right].$$

Notice that  $\gamma_x = \sin \theta \cos \phi$ ,  $\gamma_y = \sin \theta \sin \phi$ ,  $\gamma_z = \cos \theta$ , then

$$\delta u_x^{PS} = \frac{k_s^2 e^{ik_s r}}{4\pi r} \left( -\frac{\delta \rho}{\rho} \sin \theta \cos \theta \cos \phi + \frac{2\delta \mu V_s}{\mu V_P} \sin \theta \cos^2 \theta \cos \phi \right); \quad (4.5)$$

$$\delta u_y^{PS} = \frac{k_s^2 e^{ik_s r}}{4\pi r} \left( -\frac{\delta\rho}{\rho} \sin\theta \cos\theta \sin\phi + \frac{2\delta\mu V_s}{\mu V_P} \sin\theta \cos^2\theta \sin\phi \right). \quad (4.6)$$

Inserting (4.5) and (4.6) into (4.4), we get

$$\delta u_\phi^{PS} = 0,$$

i.e. the scattered S-wave is fully in the meridian plane.

#### Exercise 4.10

- (i) For scatterer  $\delta\rho$ ,  $\delta u_r^{PP} \propto \cos\theta$ ,  $\delta u_\theta^{PS} \propto \sin\theta$ , so that

$$\delta u_r^{PP} = 0 \text{ at } \theta = \pi/2; |\delta u_r^{PP}| \text{ is maximum at } \theta = 0, \pi;$$

$$\delta u_\theta^{PS} = 0 \text{ at } \theta = 0, \pi; |\delta u_\theta^{PS}| \text{ is maximum at } \theta = \pi/2.$$

- (ii) For scatterer  $\delta\lambda$ ,  $\delta u_r^{PP} \propto 1$ ,  $\delta u_\theta^{PS} \equiv 0$ . The amplitude of the scattered P wave is the same for all scattering angles. There is no scattered S wave ( $V_s = \sqrt{\mu/\rho}$ , so that S wave cannot ‘see’ the scatterer  $\delta\lambda$ ).

- (iii) For scatterer  $\delta\mu$ ,  $\delta u_r^{PP} \propto \cos^2\theta$ ,  $\delta u_\theta^{PS} \propto \sin 2\theta$ , so that

$$\delta u_r^{PP} = 0 \text{ at } \theta = \pi/2; |\delta u_r^{PP}| \text{ is maximum at } \theta = 0, \pi;$$

$$\delta u_\theta^{PS} = 0 \text{ at } \theta = 0, \pi/2, \pi; |\delta u_\theta^{PS}| \text{ is maximum at } \theta = \pi/4, 3\pi/4.$$

#### Exercise 4.11

- (a) The incoming S wave is of the form  $u_y = e^{ik_s z}$ ,  $u_x = u_z = 0$ . The far-field Green’s function of S wave excited by a force in the  $j$ -direction at  $\mathbf{r}'$  follows from (B4.10):

$$G_i^k(\mathbf{r}, \mathbf{r}', \omega) = -\frac{\gamma_i \gamma_k - \delta_{ik}}{4\pi\rho V_S^2 r} e^{ik_s r},$$

where  $r = |\mathbf{r} - \mathbf{r}'|$ . Using  $\partial'_j r = -\gamma_j$ , we find:

$$(\nabla \mathbf{u})_{kj} = \partial u_k / \partial x_j = \delta_{kx} \delta_{jz} i k_S e^{ik_s r},$$

$$\nabla \cdot \mathbf{u} = \sum_k \partial u_k / \partial x_k = 0,$$

$$(\nabla \mathbf{G})_{ikj} = \partial G_i^k / \partial x_j \approx -\frac{\gamma_i \gamma_k - \delta_{ik}}{4\pi\rho V_S^2 r} i k_S \gamma_j e^{ik_s r},$$

$$(\nabla \cdot \mathbf{G})_i = \sum_k \partial G_i^k / \partial x_k \approx -\sum_k \frac{\gamma_i \gamma_k - \delta_{ik}}{4\pi\rho V_S^2 r} i k_S \gamma_k e^{ik_s r} = 0,$$

where the ‘ $\approx$ ’ indicates that we ignore terms of  $O(r^{-2})$ .

(b) From (B4.25), ignoring the integration since we deal with point scatterers:

$$\delta u_i = \sum_k \omega^2 \delta \rho G_i^k u_k,$$

where  $u_k$  is the incoming S wave. To derive the expression for  $\delta u_r^{SS}$  we must use the Green’s function for a S wave, and to obtain the  $r$ -component we dot  $\delta u_i$  with  $\gamma_i$  to find

$$\delta u_r^{SS} = -\omega^2 \delta \rho \frac{1-1}{4\pi\rho V_S^2 r} e^{ik_S r} = 0$$

(note that the factor  $e^{ik_S z'} = 1$  since  $z' = 0$  at the scatterer by choice of the coordinate origin at the scatterer). Using the Green’s function for a scattered P wave and the same procedure we obtain

$$\delta u_r^{SP} = \omega^2 \delta \rho \frac{\gamma_y}{4\pi\rho V_P^2 r} e^{ik_P r},$$

and use  $\gamma_y = \sin \phi \sin \theta$ .

(c) The term in (B4.25) with  $\delta \lambda$  is

$$\delta u_i^{SS} = - \sum_{kj} \delta \lambda \partial'_j u_j \partial'_k G_i^k,$$

which is 0 because of the zero divergence established in (a).

(d) The term in (B4.25) with  $\delta \mu$  is

$$\delta u_i^{SS} = - \sum_{jk} \delta \mu \partial'_j G_i^k [\partial'_j u_k + \partial'_k u_j].$$

Substituting the Green’s function for the scattered S wave one finds

$$\begin{aligned} \partial'_j G_i^k [\partial'_j u_k + \partial'_k u_j] &= -\frac{k_S^2}{4\pi\rho V_S^2 r} (\gamma_i \gamma_k - \delta_{ik}) (\delta_{ky} \gamma_z + \delta_{kz} \gamma_y) \\ &= -\frac{k_S^2}{4\pi\rho V_S^2 r} (\gamma_i \gamma_y \gamma_z + \gamma_i \gamma_z \gamma_y - \delta_{iy} \gamma_z - \delta_{iz} \gamma_y), \end{aligned}$$

and substitution of  $(\gamma_x, \gamma_y, \gamma_z) = (\cos \phi \sin \theta, \sin \phi \sin \theta, \cos \theta)$  yields the requested result. The unit vectors needed to derive the individual components are:

$$\hat{e}_r = (\cos \phi \sin \theta, \sin \phi \sin \theta, \cos \theta),$$

$$\hat{e}_\phi = (-\sin \phi, \cos \phi, 0),$$

$$\hat{e}_\theta = (\cos \phi \cos \theta, \sin \phi \cos \theta, -\sin \theta).$$

(e) As in (b) and (d), but now using the expression of the Green's function for the scattered P wave.

(f) The expressions follow after dotting the results with the same unit vectors as given in (d).

## 5

### Amplitudes of body waves

**Exercise 5.1** Let the solution of (B5.3) be  $x(t) = e^{-st}$ , then  $\dot{x}(t) = -se^{-st}$ ,  $\ddot{x}(t) = s^2e^{-st}$ . Inserting them into (B5.3), we get

$$s^2 - 2\gamma s + \omega_0^2 = 0.$$

The solution of this quadratic equation is  $s = \frac{1}{2} \left( 2\gamma \pm \sqrt{4\gamma^2 - 4\omega_0^2} \right) = \gamma \pm \sqrt{\gamma^2 - \omega_0^2}$ . Usually  $\gamma \ll \omega_0$ , so  $s = \gamma \pm i\omega_1$ , where  $\omega_1 = \sqrt{\omega_0^2 - \gamma^2} > 0$ . The solution is

$$x(t) = \exp [-(\gamma \pm i\omega_1)t] = \exp (\pm i\omega_1 t - \gamma t)$$

**Exercise 5.2** Figure 5.1 compares the true  $|X(\omega)|$  and the approximation by (B5.5) for different  $\gamma$ , with  $\omega_1 = 10$  rad/s. Here  $\omega$  is between 0.3 rad/s and 30 rad/s, corresponding to a period between 0.2 s and 20 s. It is clear that the approximation is equal to the true value at  $\omega = \omega_1$ , and becomes worse as  $\omega$  moves further away from  $\omega_1$ , the natural frequency of the oscillator. The approximation is better at high frequencies than at low frequencies. As  $\gamma$  (damping) increases, the height of the peak decreases.

**Exercise 5.3** The amplitude of a wave decreases as  $\exp(-\omega t/2Q)$ , so for the same  $Q$ , the high-frequency wave damps out faster with time. This implies that with increasing travel time (distance), the seismograms are more and more dominated by low-frequency waves, and the high-frequency waves become more and more difficult to observe.

**Exercise 5.4** Dimensionless.

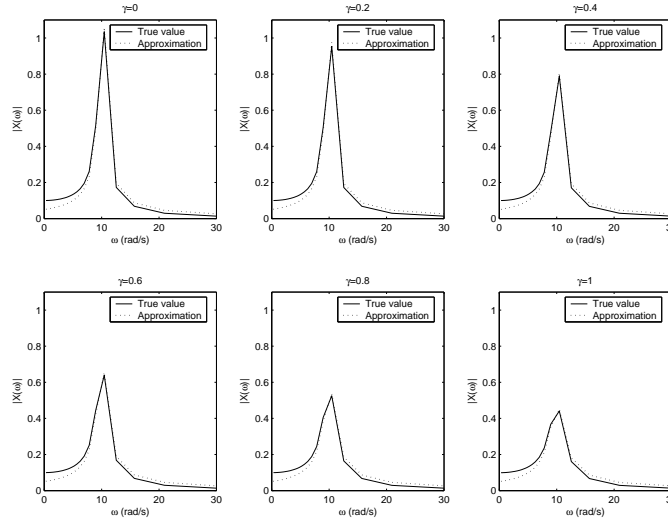


Fig. 5.1. Comparison of the true and approximate spectra for different  $\gamma$ .

**Exercise 5.5** The wave amplitude damps away as  $\exp(-kx/2Q_X)$ . Since  $k = 2\pi/\lambda$ , the shorter-wavelength wave (higher-frequency wave,  $f = c/\lambda$ ) has a larger wave number  $k$ , and thus damps away faster with distance  $x$ .

**Exercise 5.6** If a wave has an amplitude  $A \propto \exp(-kx/2Q_X)$ , its energy decreases as  $E \propto A^2 \propto \exp(-kx/Q_X)$ . Then  $dE/dx = -kE/Q_X$ , and the energy loss in one wavelength ( $dx = \lambda = 2\pi/k$ ) is  $\Delta E = |-kE dx/Q_X| = 2\pi E/Q_X$ . Thus another definition of  $Q_X$  is  $Q_X = 2\pi E/\Delta E$ , and  $2\pi/Q_X$  describes the relative energy loss per wavelength.

**Exercise 5.7** For P waves:

$$k_P = \frac{\omega}{V_P} = \omega \left[ \frac{\rho}{\kappa(\omega) + \frac{4}{3}\mu(\omega)} \right]^{\frac{1}{2}} = \frac{\omega \rho^{1/2}}{[(\text{Re}(\kappa) + \frac{4}{3}\text{Re}(\mu)) + i(\text{Im}(\kappa) + \frac{4}{3}\text{Im}(\mu))]^{1/2}}.$$

When  $|\text{Im}(\kappa)| \ll |\text{Re}(\kappa)|$  and  $|\text{Im}(\mu)| \ll |\text{Re}(\mu)|$ :

$$\begin{aligned} k_P &= \frac{\omega \rho^{1/2}}{[\text{Re}(\kappa) + \frac{4}{3}\text{Re}(\mu)]^{1/2}} \left[ 1 + \frac{i(\text{Im}(\kappa) + \frac{4}{3}\text{Im}(\mu))}{\text{Re}(\kappa) + \frac{4}{3}\text{Re}(\mu)} \right]^{-\frac{1}{2}} \\ &\approx \frac{\omega \rho^{1/2}}{[\text{Re}(\kappa) + \frac{4}{3}\text{Re}(\mu)]^{1/2}} \left[ 1 - \frac{i}{2} \frac{\text{Im}(\kappa) + \frac{4}{3}\text{Im}(\mu)}{\text{Re}(\kappa) + \frac{4}{3}\text{Re}(\mu)} \right]. \end{aligned}$$

Then from (B5.11):

$$Q_X^P = \frac{\operatorname{Re}(k_P)}{2\operatorname{Im}(k_P)} \approx -\frac{\operatorname{Re}(\kappa) + \frac{4}{3}\operatorname{Re}(\mu)}{\operatorname{Im}(\kappa) + \frac{4}{3}\operatorname{Im}(\mu)}.$$

For S waves:

$$k_S = \frac{\omega}{V_S} = \omega \left[ \frac{\rho}{\mu(\omega)} \right]^{\frac{1}{2}} = \frac{\omega\rho^{1/2}}{[\operatorname{Re}(\mu) + i\operatorname{Im}(\mu)]^{1/2}}.$$

When  $|\operatorname{Im}(\mu)| \ll |\operatorname{Re}(\mu)|$ :

$$k_S = \frac{\omega\rho^{1/2}}{[\operatorname{Re}(\mu)]^{1/2}} \left[ 1 + i\frac{\operatorname{Im}(\mu)}{\operatorname{Re}(\mu)} \right]^{-\frac{1}{2}} \approx \frac{\omega\rho^{1/2}}{[\operatorname{Re}(\mu)]^{1/2}} \left[ 1 - \frac{i}{2} \frac{\operatorname{Im}(\mu)}{\operatorname{Re}(\mu)} \right].$$

Then from (B5.11):

$$Q_X^S = \frac{\operatorname{Re}(k_S)}{2\operatorname{Im}(k_S)} \approx -\frac{\operatorname{Re}(\mu)}{\operatorname{Im}(\mu)}.$$

In the derivation above, we assume that  $|\operatorname{Im}(\kappa)| \ll |\operatorname{Re}(\kappa)|$  and  $|\operatorname{Im}(\mu)| \ll |\operatorname{Re}(\mu)|$ , which indicates that  $Q_X^P \gg 1$  and  $Q_X^S \gg 1$ . Since  $Q_X = 2\pi E/\Delta E$  (see Exercise 5.6), where  $\Delta E$  is the energy loss in one wavelength,  $Q_X \gg 1$  simply means  $\Delta E \ll E$ . Therefore the assumption we have made is consistent with the general condition  $\Delta E \ll E$ .

**Exercise 5.8** From (B5.12) and (B5.13) and the assumption that  $\operatorname{Im}(\kappa) \approx 0$ :

$$\frac{Q_X^P}{Q_X^S} = \frac{3 \operatorname{Re}(\kappa) + \frac{4}{3}\operatorname{Re}(\mu)}{4 \operatorname{Re}(\mu)}. \quad (5.1)$$

Because

$$\frac{V_P}{V_S} = \frac{[(\operatorname{Re}(\kappa) + \frac{4}{3}\operatorname{Re}(\mu))/\rho]^{1/2}}{[\operatorname{Re}(\mu)/\rho]^{1/2}} = \left[ \frac{\operatorname{Re}(\kappa) + \frac{4}{3}\operatorname{Re}(\mu)}{\operatorname{Re}(\mu)} \right]^{1/2},$$

where  $V_P$ ,  $V_S$  represent the real part of the velocity, which describes the wave propagation velocity and have nothing to do with intrinsic attenuation (imaginary part of the velocity), (5.1) becomes

$$\frac{Q_X^P}{Q_X^S} = \frac{3 V_P^2}{4 V_S^2}.$$

Hence

$$Q_X^P = \frac{3 V_P^2}{4 V_S^2} Q_X^S.$$

For a Poisson solid, where  $V_P = \sqrt{3}V_S$

$$\frac{Q_X^P}{Q_X^S} = \frac{3 V_P^2}{4 V_S^2} = \frac{3}{4} \cdot \frac{3}{1} = \frac{9}{4}.$$

**Exercise 5.9** The complex wave number of a P wave is

$$k_P = \frac{\omega}{V_P} = \frac{\omega}{\text{Re}(V_P) + i \text{Im}(V_P)} = \frac{\omega[\text{Re}(V_P) - i \text{Im}(V_P)]}{[\text{Re}(V_P)]^2 + [\text{Im}(V_P)]^2}.$$

Inserting the above equation into (B5.11):

$$Q_X^P = \frac{\text{Re}(k)}{2 \text{Im}(k)} = \frac{\text{Re}(V_P)}{-2 \text{Im}(V_P)} = -\frac{\text{Re}(V_P)}{2 \text{Im}(V_P)}.$$

Following the same procedure, we find

$$Q_X^S = -\frac{\text{Re}(V_S)}{2 \text{Im}(V_S)}.$$

## 6

### Travel times: observations

**Exercise 6.1** With 24 bit recording, the dynamic range is  $20 \log_{10} 2^{24} = 144.5$  dB. For paper recording we find  $20 \log_{10}(50/0.05) = 60$  dB. The largest recordable count is  $2^{24} = 1.68 \times 10^7$  corresponding to a displacement of  $1.68 \times 10^7 / 5000 = 3355 \mu\text{m}$  (3.3 mm).

**Exercise 6.2** A period of 24 hours corresponds to  $1.16 \times 10^{-5}$  Hz. If the seismic spectrum extends to, say, 5 Hz, the spectrum spans more than 18 octaves since  $\log_2(5/1.16 \times 10^{-5}) = 18.7$ . The dynamic range for the displacement  $u$  is of the order of  $20 \log_{10}(0.5/5 \times 10^{-9}) = 160$  dB. Since velocity  $\dot{u} \sim \omega u$  and  $\ddot{u} \sim \omega^2 u$ , for very different frequency  $\omega$ , the dynamic range for velocity and acceleration must differ from that of displacement.

**Exercise 6.3** The bandwidth of the filter is  $\Delta f = 0.15 - 0.05 = 0.1$  Hz. The window length of cross-correlation is  $T_w = 60$  s. The signal to noise ratio is  $\text{SNR}=4$ . Then from (B6.8), the Cramér-Rao lower bound estimation is

$$\sigma_{\text{CRLB}}^2 = \frac{3(1 + 2\text{SNR})}{8\pi^2 \text{SNR}^2 \Delta f^3 T_w} = \frac{3(1 + 2 \times 4)}{8\pi^2 \times 4^2 \times 0.1^3 \times 60} = 0.36 \text{ s}^2.$$

The standard deviation is  $\sigma_{\text{CRLB}} = 0.60$  s.

**Exercise 6.4** From the definition (B6.9) of  $\sigma_{\text{CPE}}$ , we have  $w = 0.1$ ,  $T_c = 10$  s,  $\sigma_{\text{CRLB}}^2 = 0.36 \text{ s}^2$ , so

$$\sigma_{\text{CPE}}^2 = wT_c^2/3 + (1 - w)\sigma_{\text{CRLB}}^2 = 0.1 \times 10^2/3 + (1 - 0.1) \times 0.36 = 3.7 \text{ s}^2.$$

The standard deviation is  $\sigma_{\text{CPE}} = 1.9$  s.

**Exercise 6.5** If SNR=20, the Cramér-Rao lower bound estimation is

$$\sigma_{CRLB}^2 = \frac{3(1 + 2\text{SNR})}{8\pi^2 \text{SNR}^2 \Delta f^3 T_w} = \frac{3(1 + 2 \times 20)}{8\pi^2 \times 20^2 \times 0.1^3 \times 60} = 0.065 \text{ s}^2.$$

The variance reduces by a factor of 5.5 (and the standard deviation, now 0.25 s, by a factor of 2.3) if the SNR increases by a factor of 5.

**Exercise 6.6** If  $\Delta f = 0.2$  Hz, the Cramér-Rao lower bound estimation is

$$\sigma_{CRLB}^2 = \frac{3(1 + 2\text{SNR})}{8\pi^2 \text{SNR}^2 \Delta f^3 T_w} = \frac{3(1 + 2 \times 4)}{8\pi^2 \times 4^2 \times 0.2^3 \times 60} = 0.045 \text{ s}^2.$$

The variance reduces by a factor of 8 if the bandwidth of the filter is doubled.

**Exercise 6.7** In VanDecar and Crosson's method, the arrival difference  $\Delta T_{ij}$  is an *estimate*, obtained from locating the time of the maximum in the cross-correlation between the seismograms at station  $i$  and station  $j$ . Because each such estimate has a different error,  $\Delta T_{ik}$  is not exactly equal to  $\Delta T_{ij} - \Delta T_{kj}$ .

# 7

## Travel times: interpretation

**Exercise 7.1** With four variables, line plots of the delay ratio as a function of only one of the four (fixing the other three) are not very informative. Better is to make contour plots of the ratio as a function of two variables, or set the ratio at a fixed level and plot a surface in 3D as a function of three variables. Here we give a solution with contour plots. It is logical to fix like variables, i.e. either  $R$  and  $S$ , or  $a$  and  $\lambda$ . One would fix  $R$  and  $S$  when one has an idea where the anomaly is located with respect to station and source and one wishes to study its resolvability as a function of its size and the seismic wavelength. Here we fix the anomaly size  $a$  and the wavelength  $\lambda$ , and study how resolvability depends on the distances.

Of course, whenever the ratio between the finite-frequency delay and the ray theoretical delay as computed from (B7.2) becomes negative, we are way beyond the validity of ray theory, the delay has completely healed and (B7.2) is not valid. So we set negative ratios to 0 and obtain the following plots:

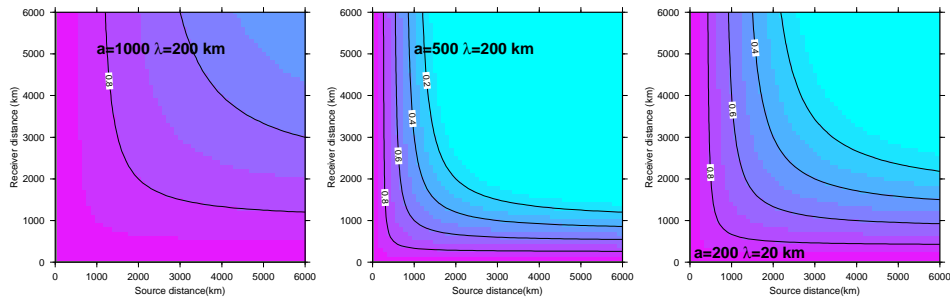


Fig. 7.1. Contour plots of (B7.2) for different  $a$  (1000, 500, and 200 km from left to right) and  $\lambda$  (200, 200, and 20 km from left to right) as a function of  $R$  and  $S$ .

**Exercise 7.2** It complicates the argument: the surface area under the acceleration wavelet is zero. Thus, the energy in the crosscorrelation is divided over both earlier and later times. To resolve the question one may generate a synthetic wavelet  $u(t)$  and crosscorrelate it with both  $u(t) + \epsilon\ddot{u}(t - \tau)$  and  $u(t) - \epsilon\ddot{u}(t - \tau)$ . This is what we did to create Figure 7.2: Indeed, the negative reflection coefficient ( $-\epsilon$ ) gives

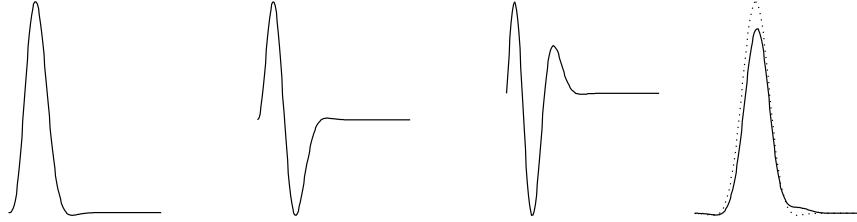


Fig. 7.2. From left to right:  $u(t)$ ,  $\dot{u}(t)$ ,  $\ddot{u}(t)$  and the crosscorrelation with a perturbed wavefield from a negative (solid line) and positive (dashed line) velocity anomaly.

a shift towards earlier time (dashed line). To create this effect we had to choose  $\epsilon$  very high. This merely shows that the effects of infinitely small point scatterers cannot be well resolved.

**Exercise 7.3** For a pulse in a narrow frequency band with dominant frequency  $\omega_0$ , we can approximate  $|\dot{m}(\omega)| \approx \delta(\omega - \omega_0)$ , and inserting this into (B7.20) we obtain

$$K_P \propto \omega_0 \sin(\omega_0 \Delta T).$$

Then the kernel has a maximum at

$$\omega_0 \Delta T = \pi/2. \tag{7.1}$$

Since  $\lambda_0 = V_P T_0 = V_P 2\pi/\omega_0$ ,

$$\omega_0 = 2\pi V_P / \lambda_0. \tag{7.2}$$

$\Delta T$  in a medium that is homogeneous everywhere except at  $x$  (Figure 7.3) is:

$$\Delta T = \frac{r_{xr} + r_{xs} - r_{rs}}{V_P} = \frac{2\sqrt{q^2 + L^2/4} - L}{V_P}. \tag{7.3}$$

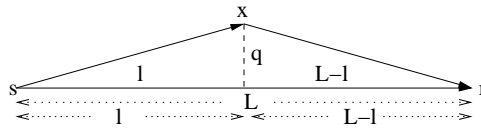


Fig. 7.3. A scatterer at point  $x$  near the central ray  $sr$  in a medium that is homogeneous everywhere except at  $x$ .

Since  $q \ll L$  (the scatterer is near the central ray),  $\sqrt{q^2 + \frac{L^2}{4}} = \frac{L}{2} \sqrt{1 + \frac{4q^2}{L^2}} \approx \frac{L}{2} \left(1 + \frac{1}{2} \frac{4q^2}{L^2}\right) = \frac{L}{2} + \frac{q^2}{L}$ , and (7.3) becomes

$$\Delta T \approx \frac{2\left(\frac{L}{2} + \frac{q^2}{L}\right) - L}{V_P} = \frac{2q^2}{LV_P}. \quad (7.4)$$

Inserting (7.2) and (7.4) into (7.1):

$$\frac{2\pi V_P}{\lambda_0} \frac{2q^2}{LV_P} = \pi/2,$$

so

$$q = \frac{\sqrt{\lambda_0 L}}{2\sqrt{2}}.$$

Since the radius of the first Fresnel zone is  $h = \sqrt{\lambda_0 L}/2$  (see (B2.48)), we have

$$q = h/\sqrt{2},$$

where  $q$  is the distance from the geometrical ray to the point of maximum kernel value.

**Exercise 7.4** A scattered SH wave coming in from the North will be visible on the EW component of the seismogram and, if it comes in early enough, will affect the reading of the SV arrival which is the one appearing on this component. From the right column of Figure B7.10, we see that such a wave can only originate from an incoming SH wave. If the Earth is isotropic and SV and SH have the same arrival time, but only the SV component is affected, this could lead to apparent anisotropy.

**Exercise 7.5** For a Ricker wavelet, (B7.30) shows that the kernel is zero when  $\Delta T = 0$ . This does not say, however, that the doughnut hole exists for all possible waveforms. The arrival time of the maximum is not causal, and a scattered wave with zero time delay could move the maximum to a different time if its waveshape is not symmetrical around zero (Exercise 7.2).

Picked onset arrival times are sensitive to scatterers on the geometrical ray. This follows from the fact that the wave  $\delta u$  from a scatterer on the geometrical ray does change the amplitude of the wave, which means it changes the time for the signal to rise above the noise level (Figure B7.12). Note, however, that this is an effect on the error in the observation, not on the arrival time itself.

**Exercise 7.6** Differentiate  $\tilde{Q}P - Q\tilde{P}$  w.r.t.  $s$ :

$$\frac{d(\tilde{Q}P - Q\tilde{P})}{ds} = \frac{d\tilde{Q}}{ds}P + \tilde{Q}\frac{dP}{ds} - \frac{dQ}{ds}\tilde{P} - Q\frac{d\tilde{P}}{ds}.$$

Both  $P$ ,  $Q$  and  $\tilde{P}$ ,  $\tilde{Q}$  satisfy the Hamiltonian system of (B3.12). Inserting (B3.12) into the above equation gives

$$\frac{d(\tilde{Q}P - Q\tilde{P})}{ds} = c\tilde{P}P + \tilde{Q}\left(-\frac{1}{c^2}VQ\right) - cP\tilde{P} - Q\left(-\frac{1}{c^2}V\tilde{Q}\right) = 0 \cdot I. \quad (7.5)$$

The last step uses the fact that  $P$ ,  $Q$ ,  $\tilde{P}$ ,  $\tilde{Q}$ ,  $V$  are diagonal for a spherically symmetric earth, and hence  $\tilde{P}P = P\tilde{P}$ ,  $\tilde{Q}VQ = QV\tilde{Q}$ .

By definition of  $P$ ,  $Q$ ,  $\tilde{P}$ ,  $\tilde{Q}$ , there is

$$\tilde{Q}P - Q\tilde{P} = \begin{pmatrix} \tilde{Q}_1P_1 - Q_1\tilde{P}_1 & 0 \\ 0 & \tilde{Q}_2P_2 - Q_2\tilde{P}_2 \end{pmatrix}. \quad (7.6)$$

Equation (7.5) implies that  $\tilde{Q}P - Q\tilde{P}$  has elements that are independent of  $s$ , and the values of these elements can be obtained from the initial conditions:  $P_1(0) = P_2(0) = \tilde{Q}_1(0) = \tilde{Q}_2(0) = 1$ ,  $\tilde{P}_1(0) = \tilde{P}_2(0) = Q_1(0) = Q_2(0) = 0$ . Now (7.6) becomes

$$\begin{aligned} \tilde{Q}P - Q\tilde{P} &= \begin{pmatrix} \tilde{Q}_1(0)P_1(0) - Q_1(0)\tilde{P}_1(0) & 0 \\ 0 & \tilde{Q}_2(0)P_2(0) - Q_2(0)\tilde{P}_2(0) \end{pmatrix} \\ &= \begin{pmatrix} 1 & 0 \\ 0 & 1 \end{pmatrix} = I. \end{aligned} \quad (7.7)$$

Thus, we have proved the first equality in (B7.32). The proof of the second equality in (B7.32) is very similar.

**Exercise 7.7** In a homogeneous medium, for a point  $\mathbf{x} = (l, q_1, q_2)$  in the ray coordinate system, the ray length is  $|\mathbf{x}| = \sqrt{l^2 + q_1^2 + q_2^2}$ . The travel time  $T$  satisfies  $cT = |\mathbf{x}|$ . Since  $q_1^2 + q_2^2 \ll l^2$ , we have

$$cT = |\mathbf{x}| = \sqrt{l^2 + q_1^2 + q_2^2} = l\sqrt{1 + \frac{q_1^2 + q_2^2}{l^2}} \approx l + \frac{q_1^2 + q_2^2}{2l}. \quad (7.8)$$

In order to use (B7.33), we need to know every parameter on the left hand side of this equation. The central ray and scattered rays in a homogeneous medium are shown in Figure 7.3. We have  $V_r = c$ ,  $\mathcal{R}_{rs} = L$ . From (7.8), we have

$$\mathcal{R}_{xs} = l + \frac{q^2}{2l}, \quad \mathcal{R}_{xr} = (L - l) + \frac{q^2}{2(L - l)},$$

where  $q^2 = q_1^2 + q_2^2$ . Then

$$\sqrt{|\det(\mathbf{H}_{xs} + \mathbf{H}_{xr})|} = \frac{\mathcal{R}_{rs}}{V_r \mathcal{R}_{xs} \mathcal{R}_{xr}} = \frac{L}{c[l + \frac{q^2}{2l}][L - l + \frac{q^2}{2(L-l)}}.$$

Ignoring the terms of  $q^2$  and higher order in the denominator, we get

$$\sqrt{|\det(\mathbf{H}_{xs} + \mathbf{H}_{xr})|} = \frac{1}{c} \cdot \frac{L}{l(L-l)} = \frac{1}{c} \left| \frac{1}{l} + \frac{1}{L-l} \right|.$$

**Exercise 7.8** The Maslov index is equal to the number of dimensions lost by the bundle of rays. In a 3-D medium, the maximum possible number of lost dimensions is 2, i.e. when a 3-D bundle of rays focuses in a single point. Therefore, the possible values of the Maslov index is: 0 (e.g. P, pP, no caustic); 1 (e.g. PP, SS, at the caustic, which forms a line for different azimuths); 2 (e.g. PP, PKP, and multiple surface reflected waves that focus to a point at the antipode of the source). The increase of the Maslov index  $\Delta M$  can accumulate to a large number as a multiply reflected ray bundle passes through successive caustics. While this may seem at odds with the fact that  $\mathbf{H}$  is only a  $2 \times 2$  matrix so that  $\text{sig}(\mathbf{H})$  can never exceed  $\pm 2$ , the harmonic nature of its effect, e.g. in (B7.28), makes that an index equal to 3 has the same effect as an index equal to -1, so that  $\text{sig}(\mathbf{H})$  can still be used even in the case of multiple caustics.

## 8

### Body wave amplitudes: Observation and interpretation

#### Exercise 8.1

$$\begin{aligned}
 A + \delta A &= \sqrt{\frac{1}{T_p} \int_0^{T_p} [u(t) + \delta u(t)]^2 dt} \\
 &= \sqrt{\frac{1}{T_p} \int_0^{T_p} u^2(t) \left[1 + \frac{\delta u(t)}{u(t)}\right]^2 dt} \\
 &\approx \sqrt{\frac{1}{T_p} \int_0^{T_p} u^2(t) \left[1 + \frac{2\delta u(t)}{u(t)}\right] dt} \\
 &= \sqrt{\frac{1}{T_p} \int_0^{T_p} u^2(t) dt + \frac{1}{T_p} \int_0^{T_p} \frac{2\delta u(t)}{u(t)} dt} \\
 &= \sqrt{\frac{1}{T_p} \int_0^{T_p} u^2(t) dt} \sqrt{1 + \frac{\frac{1}{T_p} \int_0^{T_p} 2\delta u(t) u(t) dt}{\frac{1}{T_p} \int_0^{T_p} u^2(t) dt}} \\
 &\approx \sqrt{\frac{1}{T_p} \int_0^{T_p} u(t)^2 dt} \left(1 + \frac{\int_0^{T_p} u(t) \delta u(t) dt}{\int_0^{T_p} u(t)^2 dt}\right). \tag{8.1}
 \end{aligned}$$

**Exercise 8.2** The attenuation kernel does have a doughnut hole. This is easy to see from the expression of the attenuation kernel (B8.14), which has a sine dependence on the detour time  $\Delta T$  as the travel time kernel does. For a scatterer on the geometrical ray,  $\Delta T = 0$  (assuming  $\Delta\Phi = 0$ ), so  $K_X^Q = 0$ , which gives the doughnut hole of zero sensitivity.

The focusing kernel does not have a doughnut hole. From the expression of the

focusing kernel (B8.8),  $K_X^A$  has a cosine dependence on the detour time  $\Delta T$ . For a scatterer on the geometrical ray,  $\Delta T = 0$  (assuming  $\Delta\Phi = 0$ ), so  $K_X^Q$  is maximum, which means that the largest focusing effect on amplitudes is from scatterers on the geometrical ray.

Of course, if the Maslov index is equal to 1, the situation is the reverse.

## 9

### Normal modes

**Exercise 9.1** To save on notation we adopt the Einstein summation notation, in which a summation is implied over every index that occurs twice in one term, i.e.  $a_i b_i$  means  $\sum_i a_i b_i$ . In Cartesian coordinates:

$$\begin{aligned} (\mathcal{L}u, v) &= \int_V (\mathcal{L}u)_i v_i^* d^3\mathbf{r} = \int_V \frac{\partial}{\partial x_j} \left( c_{ijkl} \frac{\partial u_l}{\partial x_k} \right) v_i^* d^3\mathbf{r} \\ &= \int_V \frac{\partial}{\partial x_j} \left( c_{ijkl} \frac{\partial u_l}{\partial x_k} v_i^* \right) d^3\mathbf{r} - \int_V c_{ijkl} \frac{\partial u_l}{\partial x_k} \frac{\partial v_i^*}{\partial x_j} d^3\mathbf{r}. \end{aligned} \quad (9.1)$$

Apply Gauss's theorem to the first term on the right hand side of (9.1):

$$\int_V \frac{\partial}{\partial x_j} \left( c_{ijkl} \frac{\partial u_l}{\partial x_k} v_i^* \right) d^3\mathbf{r} = \int_S c_{ijkl} \frac{\partial u_l}{\partial x_k} v_i^* n_j d^2\mathbf{r}, \quad (9.2)$$

where  $V$  is the Earth and  $S$  its surface, and  $\mathbf{n}$  is a unit normal vector of  $S$ . Notice that  $\sigma_{ij} = c_{ijkl} \frac{\partial u_l}{\partial x_k}$ , and the traction  $\mathbf{F}$  on  $S$  is  $F_i = \sigma_{ij} n_j$ , so (9.2) becomes

$$\int_V \frac{\partial}{\partial x_j} \left( c_{ijkl} \frac{\partial u_l}{\partial x_k} v_i^* \right) d^3\mathbf{r} = \int_S \sigma_{ij} v_i^* n_j d^2\mathbf{r} = \int_S F_i v_i^* d^2\mathbf{r} = 0,$$

because  $S$  is a free surface on which  $\mathbf{F} = \mathbf{0}$ . Substituting this into (9.1), we get

$$(\mathcal{L}u, v) = - \int_V c_{ijkl} \frac{\partial u_l}{\partial x_k} \frac{\partial v_i^*}{\partial x_j} d^3\mathbf{r}. \quad (9.3)$$

Similarly,

$$\begin{aligned} (u, \mathcal{L}v) &= \int_V u_i (\mathcal{L}v^*)_i d^3\mathbf{r} = \int_V u_i \frac{\partial}{\partial x_j} \left( c_{ijkl} \frac{\partial v_l^*}{\partial x_k} \right) d^3\mathbf{r} \\ &= \int_V \frac{\partial}{\partial x_j} \left( c_{ijkl} u_i \frac{\partial v_l^*}{\partial x_k} \right) d^3\mathbf{r} - \int_V c_{ijkl} \frac{\partial u_i}{\partial x_j} \frac{\partial v_l^*}{\partial x_k} d^3\mathbf{r}. \end{aligned} \quad (9.4)$$

Apply Gauss's theorem to the first term on the right hand side of (9.4):

$$\int_V \frac{\partial}{\partial x_j} \left( c_{ijkl} u_i \frac{\partial v_l^*}{\partial x_k} \right) d^3 \mathbf{r} = \int_S c_{ijkl} u_i \frac{\partial v_l^*}{\partial x_k} n_j d^2 \mathbf{r} \quad (9.5)$$

Again because of the zero traction on the boundary  $S$ :

$$\int_V \frac{\partial}{\partial x_j} \left( c_{ijkl} u_i \frac{\partial v_l^*}{\partial x_k} \right) d^3 \mathbf{r} = \int_S u_i \sigma_{ij}^* n_j d^2 \mathbf{r} = \int_S u_i F_i^* d^2 \mathbf{r} = 0.$$

Substituting this into (9.4), we get

$$(u, \mathcal{L}v) = - \int_V c_{ijkl} \frac{\partial u_i}{\partial x_j} \frac{\partial v_l^*}{\partial x_k} d^3 \mathbf{r} = - \int_V c_{lkji} \frac{\partial u_i}{\partial x_j} \frac{\partial v_l^*}{\partial x_k} d^3 \mathbf{r}, \quad (9.6)$$

the last step uses the symmetry properties of the elastic tensor:  $c_{ijkl} = c_{klij} = c_{lkji}$ . Because  $i, j, k, l$  in (9.6) are dummy subscripts, we can rearrange them ( $l \rightarrow i, k \rightarrow j, j \rightarrow k, i \rightarrow l$ ), and (9.6) becomes

$$(u, \mathcal{L}v) = - \int_V c_{ijkl} \frac{\partial u_l}{\partial x_k} \frac{\partial v_i^*}{\partial x_j} d^3 \mathbf{r}. \quad (9.7)$$

Compare (9.3) and (9.7), we get

$$(\mathcal{L}u, v) = (u, \mathcal{L}v),$$

which establishes that  $\mathcal{L}$  is Hermitian.

**Exercise 9.2** From (B9.11):  $(\mathbf{u}_p, \mathcal{L}\mathbf{u}_q) = (\mathcal{L}\mathbf{u}_p, \mathbf{u}_q)$ . Using (B9.1) without a force (such that it is a free oscillation and  $\omega$  is an eigenfrequency):

$$(\omega_q^2)^* (\mathbf{u}_p, \rho \mathbf{u}_q) = \omega_p^2 (\rho \mathbf{u}_p, \mathbf{u}_q).$$

Since  $\rho$  is real,  $(\mathbf{u}_p, \rho \mathbf{u}_q) = (\rho \mathbf{u}_p, \mathbf{u}_q)$ . The above equation becomes

$$[\omega_p^2 - (\omega_q^2)^*] (\mathbf{u}_p, \rho \mathbf{u}_q) = 0.$$

If  $\omega_p \neq \omega_q$ , then it must be that  $(\mathbf{u}_p, \rho \mathbf{u}_q) = 0$ , i.e. eigenvectors belonging to different eigenvalues are orthogonal. If  $\omega_p = \omega_q$ , then  $(\mathbf{u}_p, \rho \mathbf{u}_q) = |\mathbf{u}_p|^2 \neq 0$ , so  $(\omega_q^2)^* = \omega_q^2$ , i.e.  $\omega^2$  must be real.

**Exercise 9.3** Working out the variations and collecting terms with  $\delta V_P, \delta V_S$  and

$\delta\rho$  gives

$$\begin{aligned}
& K_\kappa \delta\kappa + K_\mu \delta\mu + K'_\rho \delta\rho \\
&= K_\kappa [\delta\rho (V_P^2 - \frac{4}{3}V_S^2) - \frac{8\rho}{3}V_S \delta V_S + 2\rho V_P \delta V_P] \\
&+ K_\mu [2\rho V_S \delta V_S + V_S^2 \delta\rho] \\
&+ K'_\rho \delta\rho \\
&= 2\rho V_P K_\kappa \delta V_P \\
&+ 2\rho V_S (K_\mu - \frac{4}{3}K_\kappa) \delta V_S \\
&+ [(V_P^2 - \frac{4}{3}V_S^2)K_\kappa + V_S^2 K_\mu + K'_\rho] \delta\rho,
\end{aligned}$$

which equals the conversion factors in Table B9.2 because  $(V_P^2 - \frac{4}{3}V_S^2) = \kappa/\rho$ .

**Exercise 9.4** Since the angular order  $s = 0$  gives the case for spherical symmetry (remember that the azimuthal order  $|m| \leq s$  so that  $m \equiv 0$ ), one expects that the kernels reduce to the partial derivatives known from the spherically symmetric case.

**Exercise 9.5** Starting from the right hand side:

$$\begin{aligned}
(e^{-it\mathbf{H}})_{m'm} &= (\mathbf{I} - it\mathbf{H} + \frac{1}{2}(it)^2\mathbf{H}^2 - \dots)_{m'm} \\
&= \delta_{m'm} - itH_{m'm} + \frac{1}{2}(it)^2 \sum_k H_{m'k}H_{km} - \dots
\end{aligned}$$

We may replace  $\delta_{m'm}$  by  $\sum_j Z_{m'j}Z_{mj}^*$  because of the orthogonality (B9.22). Inserting the expression for the elements of  $\mathbf{H}$ :

$$\begin{aligned}
& (e^{-it\mathbf{H}})_{m'm} \\
&= \sum_j [Z_{m'j}Z_{mj}^* - itZ_{m'j}\delta\omega_j Z_{mj}^* + \frac{1}{2}(it)^2 \sum_{ik} Z_{m'j}\delta\omega_j Z_{kj}^* Z_{ki}\delta\omega_i Z_{mi}^* - \dots] \\
&= \sum_j [Z_{m'j}Z_{mj}^* - itZ_{m'j}\delta\omega_j Z_{mj}^* + \frac{1}{2}(it)^2 \sum_i Z_{m'j}\delta\omega_j \delta_{ij}\delta\omega_i Z_{mi}^* - \dots] \\
&= \sum_j Z_{m'j} [1 - it\delta\omega_j + \frac{1}{2}(it)^2 \delta\omega_j^2 - \dots] Z_{mj}^* \\
&= \sum_j Z_{mj}^* e^{-i\delta\omega_j t} Z_{m'j}.
\end{aligned}$$

**Exercise 9.6** With  $P = \exp[i\delta t H]$  and using a Taylor expansion:

$$\begin{aligned} PZ &= Z - i\delta t HZ + (i\delta t)^2 H^2 Z - \dots \\ &= Z - i\delta t Z\Omega + (i\delta t)^2 Z\Omega^2 - \dots \\ &= Z[I - i\delta t\Omega + (i\delta t)^2\Omega^2 - \dots] \\ &= Z \exp[-i\delta t\Omega]. \end{aligned}$$

Then  $D = Z^{-1}PZ = \exp[-i\delta t\Omega]$ .

# 10

## Surface wave interpretation: ray theory

**Exercise 10.1** The phase velocity  $C_n(\omega) = \omega/k_n(\omega) = c_n$ . Taking  $k$  as the independent variable, we get  $\omega_n(k) = c_n k$ . Then the group velocity  $\mathcal{U}_n(k) = d\omega_n(k)/dk = c_n$ . Hence, if there is no dispersion, the group velocity and the phase velocity are the same, and both are independent of frequency.

**Exercise 10.2** If the phase velocity satisfies

$$C_n(\omega) = \frac{\omega}{k_n(\omega)} = c_0 + \frac{a}{\omega}, \quad (10.1)$$

then

$$\frac{dk_n(\omega)}{d\omega} = \frac{2\omega}{c_0\omega + a} - \frac{c_0\omega^2}{(c_0\omega + a)^2} = \frac{\omega(c_0\omega + 2a)}{(c_0\omega + a)^2}.$$

Taking  $k$  as the independent variable, we get the group velocity

$$\mathcal{U}_n = \frac{d\omega}{dk} = \left(\frac{dk}{d\omega}\right)^{-1} = \frac{(c_0\omega + a)^2}{\omega(c_0\omega + 2a)}.$$

In order to compare the phase velocity and the group velocity, we take their ratio

$$\frac{\mathcal{U}_n}{C_n} = \frac{c_0\omega + a}{c_0\omega + 2a} = 1 - \frac{a}{c_0\omega + 2a}. \quad (10.2)$$

Since  $a > 0$  (see the slope in Figure B10.3), (10.2) indicates that  $\mathcal{U}_n/C_n < 1$ , i.e.  $\mathcal{U}_n < C_n$ .

In Figure B10.3, for the first higher mode near a period  $T$  of 50 s,  $C_n \approx 5.0$  km/s, the slope  $dC_n/dT \approx 0.015$  km/s<sup>2</sup>, the intercept is about 4.3 km/s, and  $\omega = 2\pi/T \approx 0.1257$  rad/s. Then in (10.1):

$$a = \frac{dC_n}{d(\frac{1}{\omega})} = 2\pi \frac{dC_n}{dT} = 2\pi \times 0.015 \approx 0.094 \text{ km/s, and } c_0 = 4.3 \text{ km/s.}$$

Substituting all these numbers into (10.2), we get

$$\frac{U_n}{C_n} = 1 - \frac{0.094}{4.3 \times 0.1257 + 2 \times 0.094} \approx 0.871,$$

and the group velocity  $U_n \approx 0.871C_n \approx 0.871 \times 5.0 \approx 4.4$  km/s.

**Exercise 10.3** For body waves, the ray parameter  $p = r \sin i/v$ . For an SSSS wave,  $p_1 = r_1/v_1$ , if point 1 is the bottoming point ( $i_1 = 90^\circ$ ) of the S leg in the mantle. For an ScS wave,  $p_2 = r_2 \sin i_2/v_2$ , taking point 2 the reflecting point at the core-mantle boundary. It's obvious that  $r_1 > r_2$ ,  $v_1 < v_2$ ,  $i_1 = 90^\circ > i_2$ , so  $p_1 > p_2$ . The equivalent phase velocity  $C_n$  of these body waves is related to  $p$  through  $p = a/C_n$ , where  $a$  is the radius of the earth. Thus we have  $C_{n1} < C_{n2}$ , i.e. the ScS wave has the higher equivalent phase velocity.

The equivalent group velocity of a body wave can be written as  $U_n = a\Delta/T$ , where  $a$  is the radius of the earth,  $\Delta$  is the epicentral distance in radian,  $T$  is the actual travel time of wave energy, i.e. the travel time of the body wave. Depending on the epicentral distance  $\Delta$ , the SSSS wave may arrive earlier (at close distance) or later than the ScS wave, and thus may have a higher or lower group velocity.

**Exercise 10.4** The body wave phase velocity (apparent velocity)  $C_n$  and the body wave group velocity  $V_s$  are related by (B10.9):

$$C_n(\omega) = \frac{a}{r_b} V_s(r_b).$$

Since  $a = 6371$  km (the earth's radius),  $r_b = 5961$  km (the radius of the 410 km discontinuity), and  $V_s(r_b) = 5.08$  km/s:

$$C_n = 5.08 \times 6371/5961 \approx 5.43 \text{ km/s}.$$

For a phase velocity  $C_n$  less than 5.43 km/s the surface wave modes will become evanescent below 410 km depth.

From Figure B10.3 we see that both the first higher Rayleigh and Love mode become evanescent at a period of about 70 s, but very high modes ( $n > 8$ ) remain oscillatory even at a period of 10 s. From Figure B6.8 this is a mostly a low noise region on Earth.

**Exercise 10.5** Expanding  $\tilde{g}_i(r)$  in terms of the basis  $\{g_k(r)\}$  for  $k = 1, \dots, M$ :

$$\tilde{g}_i(r) = \sum_{k=1}^M a_{ik} g_k(r). \quad (10.3)$$

In order to determine the coefficients  $a_{ik}$ , substitute (10.3) into the orthogonality

condition

$$\int_0^a \tilde{\mathbf{g}}_i(r) \cdot \mathbf{g}_j(r) \mathbf{d}r = \delta_{ij},$$

and switch the order of integral and sum, we get

$$\sum_{k=1}^M a_{ik} \int_0^a \mathbf{g}_k(r) \cdot \mathbf{g}_j(r) \mathbf{d}r = \delta_{ij}.$$

This can be written as

$$\sum_{k=1}^M a_{ik} G_{kj} = \delta_{ij}, \quad (10.4)$$

where  $G_{kj} = \int_0^a \mathbf{g}_k(r) \cdot \mathbf{g}_j(r) \mathbf{d}r$ . For each fixed  $i$ , (10.4) can be written as

$$\mathbf{G}\mathbf{a} = \mathbf{d}, \quad (10.5)$$

where  $\mathbf{G} = \{G_{jk}\} = \{G_{kj}\}$ ,  $\mathbf{a} = (a_{i1}, a_{i2}, \dots, a_{iM})^T$ ,  $\mathbf{d} = (\delta_{i1}, \delta_{i2}, \dots, \delta_{iM})^T$ . Solving (10.5) for each  $i$  gives the coefficients  $a_{ik}$ , and by (10.3), the dual basis  $\tilde{\mathbf{g}}_i(r)$ .

# 11

## Surface waves: Finite frequency theory

**Exercise 11.1** Let  $u_0$  be the unperturbed wave with zero phase, and the corresponding perturbation is  $\delta u_0$ . If the unperturbed wave has a nonzero phase  $\phi_0$ , we can view this as a time shift, which is the same for both unperturbed wave and the perturbation. We therefore write  $u = u_0 e^{i\phi_0}$  and  $\delta u = \delta u_0 e^{i\phi_0}$ . Insert  $u$  and  $\delta u$  into (B11.2) and (B11.3):

$$\delta\phi = \text{Im}\left(\frac{\delta u}{u}\right) = \text{Im}\left(\frac{\delta u_0 e^{i\phi_0}}{u_0 e^{i\phi_0}}\right) = \text{Im}\left(\frac{\delta u_0}{u_0}\right).$$

$$\delta \ln A = \text{Re}\left(\frac{\delta u}{u}\right) = \text{Re}\left(\frac{\delta u_0 e^{i\phi_0}}{u_0 e^{i\phi_0}}\right) = \text{Re}\left(\frac{\delta u_0}{u_0}\right).$$

Therefore, (B11.2) and (B11.3) remain correct for  $u$  with nonzero phase.

**Exercise 11.2** The boxcar window is

$$w(t) = \begin{cases} 1 & \text{if } -T/2 \leq t < T/2 \\ 0 & \text{otherwise} \end{cases}.$$

Its spectrum is

$$\begin{aligned} W(\omega) &= \int_{-\infty}^{+\infty} w(t) e^{i\omega t} dt = \int_{-T/2}^{T/2} e^{i\omega t} dt = \frac{1}{i\omega} \left( e^{i\omega T/2} - e^{-i\omega T/2} \right) \\ &= \frac{2}{\omega} \sin \frac{\omega T}{2} = T \text{sinc} \left( \frac{\omega T}{2} \right), \end{aligned} \quad (11.1)$$

where  $\text{sinc}(x) = \sin(x)/x$ . Its power spectrum is

$$P(\omega) = |W(\omega)|^2 = T^2 \text{sinc}^2 \left( \frac{\omega T}{2} \right).$$

The first column of Figure 11.1 plots  $w(t)$ ,  $W(\omega)$  and  $P(\omega)$  of a boxcar window.

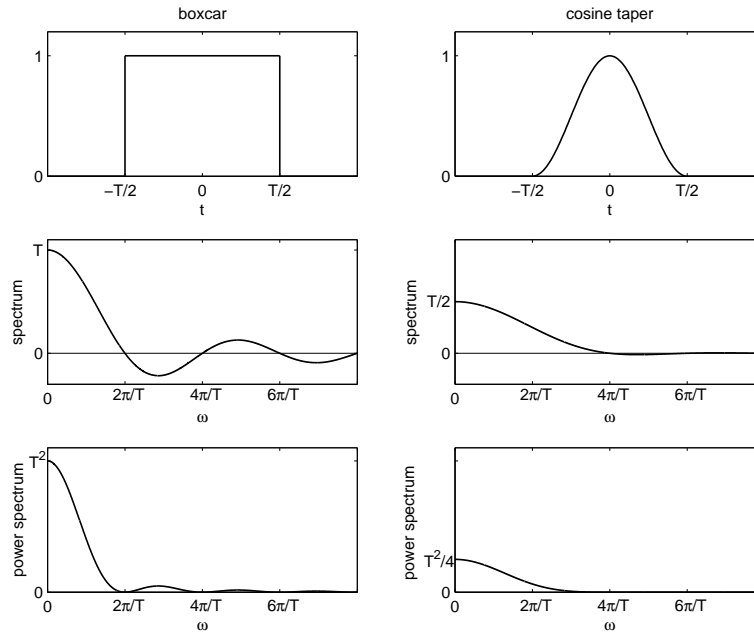


Fig. 11.1. Time series, spectrum, and power spectrum of a boxcar window (left) and a cosine taper (right).

**Exercise 11.3** A cosine taper between  $-T/2 \leq t < T/2$  is given by

$$w(t) = \begin{cases} \frac{1}{2} \left( 1 - \cos \frac{2\pi(t+T/2)}{T} \right) & \text{if } -T/2 \leq t < T/2 \\ 0 & \text{otherwise} \end{cases}.$$

Its spectrum is

$$\begin{aligned} W(\omega) &= \int_{-\infty}^{+\infty} w(t) e^{i\omega t} dt = \int_{-T/2}^{T/2} \frac{1}{2} \left( 1 - \cos \frac{2\pi(t+T/2)}{T} \right) e^{i\omega t} dt \\ &= \frac{1}{2} \int_{-T/2}^{T/2} e^{i\omega t} dt - \frac{1}{2} \int_{-T/2}^{T/2} \cos \frac{2\pi(t+T/2)}{T} e^{i\omega t} dt \\ &= \frac{T}{2} \operatorname{sinc}\left(\frac{\omega T}{2}\right) - \frac{1}{2} I. \end{aligned} \quad (11.2)$$

In the last step, we use (11.1) to get the first term in (11.2). Now we compute the

second integral in (11.2):

$$\begin{aligned}
I &= \int_{-T/2}^{T/2} \cos \frac{2\pi(t+T/2)}{T} e^{i\omega t} dt \\
&= \frac{1}{i\omega} \int_{-T/2}^{T/2} \cos \frac{2\pi(t+T/2)}{T} d(e^{i\omega t}) \\
&= \frac{1}{i\omega} \left[ \cos \frac{2\pi(t+T/2)}{T} e^{i\omega t} \Big|_{-T/2}^{T/2} - \frac{2\pi}{T} \int_{-T/2}^{T/2} \sin \frac{2\pi(t+T/2)}{T} e^{i\omega t} dt \right] \\
&= \frac{1}{i\omega} \left[ e^{i\frac{\omega T}{2}} - e^{-i\frac{\omega T}{2}} - \frac{2\pi}{i\omega T} \int_{-T/2}^{T/2} \sin \frac{2\pi(t+T/2)}{T} d(e^{i\omega t}) \right] \\
&= \frac{2}{\omega} \sin(\omega T/2) + \frac{2\pi}{T\omega^2} \left[ \sin \frac{2\pi(t+T/2)}{T} e^{i\omega t} \Big|_{-T/2}^{T/2} \right. \\
&\quad \left. + \frac{2\pi}{T} \int_{-T/2}^{T/2} \cos \frac{2\pi(t+T/2)}{T} e^{i\omega t} dt \right] \\
&= T \operatorname{sinc} \left( \frac{\omega T}{2} \right) + \left( \frac{2\pi}{\omega T} \right)^2 I.
\end{aligned}$$

Solving the above equation for the integral  $I$  gives

$$I = \frac{\omega^2 T^3}{\omega^2 T^2 - 4\pi^2} \operatorname{sinc} \left( \frac{\omega T}{2} \right).$$

Inserting this into (11.2), we get the spectrum of the cosine taper

$$W(\omega) = \frac{T}{2} \operatorname{sinc} \left( \frac{\omega T}{2} \right) - \frac{1}{2} \frac{\omega^2 T^3}{\omega^2 T^2 - 4\pi^2} \operatorname{sinc} \left( \frac{\omega T}{2} \right) = \frac{2\pi^2 T}{4\pi^2 - \omega^2 T^2} \operatorname{sinc} \left( \frac{\omega T}{2} \right).$$

The power spectrum of the cosine taper is

$$P(\omega) = |W(\omega)|^2 = \frac{4\pi^4 T^2}{4\pi^2 - \omega^2 T^2} \operatorname{sinc} \left( \frac{\omega T}{2} \right).$$

The second column of 11.1 plots  $w(t)$ ,  $W(\omega)$  and  $P(\omega)$  of the cosine taper.

Comparison of the spectra of the two windows shows that the boxcar window has a narrower peak (more delta-function shaped), but larger sidelobes spreading a broader range of frequencies. On the other hand, the cosine tapered window has very small sidelobes at the expense of a somewhat broader central peak.

## 12

### Model parametrization

**Exercise 12.1** We know that the radial functions are orthogonal:

$$\int_0^a f_k(r) f_{k'}(r) r^2 dr = \delta_{kk'}, \quad (12.1)$$

and the angular functions are orthogonal:

$$\int_0^\pi X_l^m(\theta) X_{l'}^{m'}(\theta) \sin \theta d\theta = \frac{1}{2\pi} \delta_{ll'}. \quad (12.2)$$

The orthogonal condition of basis functions  $h_{klm}(r, \theta, \phi)$  is

$$I = \int_0^a \int_0^\pi \int_0^{2\pi} h_{klm}(r, \theta, \phi) h_{k'l'm'}(r, \theta, \phi) r^2 \sin \theta dr d\theta d\phi = \delta_{kk'} \delta_{ll'} \delta_{mm'}. \quad (12.3)$$

Rewrite (B12.3) as

$$h_{klm}(r, \theta, \phi) = f_k(r) X_l^{|m|}(\theta) \Phi_m(\phi), \quad (12.4)$$

where

$$\Phi_m(\phi) = \begin{cases} \sqrt{2} \cos m\phi & -l \leq m < 0 \\ 1 & m = 0 \\ \sqrt{2} \sin m\phi & 0 < m \leq l \end{cases}. \quad (12.5)$$

Insert (12.4) into (12.3) and apply (12.1)-(12.2):

$$\begin{aligned} I &= \int_0^a \int_0^\pi \int_0^{2\pi} f_k(r) X_l^{|m|}(\theta) \Phi_m(\phi) f_{k'}(r) X_{l'}^{|m'|}(\theta) \Phi_{m'}(\phi) r^2 \sin \theta dr d\theta d\phi \\ &= \int_0^a f_k(r) f_{k'}(r) r^2 dr \int_0^\pi X_l^{|m|}(\theta) X_{l'}^{|m'|}(\theta) \sin \theta d\theta \int_0^{2\pi} \Phi_m(\phi) \Phi_{m'}(\phi) d\phi \\ &= \delta_{kk'} \delta_{ll'} \frac{1}{2\pi} \int_0^{2\pi} \Phi_m(\phi) \Phi_{m'}(\phi) d\phi. \end{aligned} \quad (12.6)$$

Comparison of (12.6) and (12.3) shows that we only need to prove

$$I_1 = \frac{1}{2\pi} \int_0^{2\pi} \Phi_m(\phi) \Phi_{m'}(\phi) d\phi = \delta_{mm'}. \quad (12.7)$$

Since (12.5) shows that  $\Phi_m(\phi)$  has different expressions depending on the value of  $m$ , we shall prove (12.7) for each combination separately. Also notice that  $m$  and  $m'$  are symmetric in (12.7).

(i)  $m = m' = 0$

$$I_1 = \frac{1}{2\pi} \int_0^{2\pi} 1 \times 1 \times d\phi = 1 = \delta_{mm'}.$$

(ii)  $m = 0, -l \leq m' < 0$  (or  $-l \leq m < 0, m' = 0$ )

$$I_1 = \frac{1}{2\pi} \int_0^{2\pi} \sqrt{2} \cos m' \phi d\phi = 0 = \delta_{mm'}.$$

(iii)  $m = 0, 0 < m' \leq l$  (or  $0 < m \leq l, m' = 0$ )

$$I_1 = \frac{1}{2\pi} \int_0^{2\pi} \sqrt{2} \sin m' \phi d\phi = 0 = \delta_{mm'}.$$

(iv)  $-l \leq m < 0, -l \leq m' < 0$

$$\begin{aligned} I_1 &= \frac{1}{2\pi} \int_0^{2\pi} \sqrt{2} \cos m\phi \sqrt{2} \cos m'\phi d\phi \\ &= \frac{1}{2\pi} \int_0^{2\pi} [\cos(m+m')\phi + \cos(m-m')\phi] d\phi \\ &= \frac{1}{2\pi} \int_0^{2\pi} \cos(m-m')\phi d\phi. \end{aligned}$$

If  $m = m'$

$$I_1 = \frac{1}{2\pi} \int_0^{2\pi} d\phi = 1 = \delta_{mm'}.$$

If  $m \neq m'$

$$I_1 = \frac{1}{2\pi(m-m')} \sin(m-m')\phi \Big|_0^{2\pi} = 0 = \delta_{mm'}.$$

(v)  $-l \leq m < 0$ ,  $0 < m' \leq l$  (or  $0 < m \leq l$ ,  $-l \leq m' < 0$ )

$$\begin{aligned}
 I_1 &= \frac{1}{2\pi} \int_0^{2\pi} \sqrt{2} \cos m\phi \sqrt{2} \sin m'\phi d\phi \\
 &= \frac{1}{2\pi} \int_0^{2\pi} [\sin(m+m')\phi - \sin(m-m')\phi] d\phi \\
 &= \frac{1}{2\pi} \left[ \frac{-1}{m+m'} \cos(m+m')\phi + \frac{1}{m-m'} \cos(m-m')\phi \right]_0^{2\pi} \quad (\text{since } m \neq m') \\
 &= 0 = \delta_{mm'}.
 \end{aligned}$$

(vi)  $0 < m \leq l$ ,  $0 < m' \leq l$

$$\begin{aligned}
 I_1 &= \frac{1}{2\pi} \int_0^{2\pi} \sqrt{2} \sin m\phi \sqrt{2} \sin m'\phi d\phi \\
 &= \frac{1}{2\pi} \int_0^{2\pi} [-\cos(m+m')\phi + \cos(m-m')\phi] d\phi \\
 &= \frac{1}{2\pi} \int_0^{2\pi} \cos(m-m')\phi d\phi \\
 &= \delta_{mm'}.
 \end{aligned}$$

The last step uses the result in 4.

Thus, we have proved (12.7). Inserting (12.7) into (12.6) gives (12.3), i.e. the basis defined by (B12.2) is orthogonal.

**Exercise 12.2** The basis  $h_k(\mathbf{r})$  is orthogonal means

$$\int_V h_k(\mathbf{r}) h_l(\mathbf{r}) d^3\mathbf{r} = \delta_{kl}, \quad (12.8)$$

where  $V$  is the volume over which the basis is defined. Expand the model  $m(\mathbf{r})$  into the basis  $h_k(\mathbf{r})$ :

$$m(\mathbf{r}) = \sum_k a_k h_k(\mathbf{r}). \quad (12.9)$$

Multiply both sides of (12.9) by  $h_l(\mathbf{r})$  and integrate over  $V$ :

$$\int_V m(\mathbf{r}) h_l(\mathbf{r}) d^3\mathbf{r} = \int_V \left( \sum_k a_k h_k(\mathbf{r}) \right) h_l(\mathbf{r}) d^3\mathbf{r} = \sum_k a_k \int_V h_k(\mathbf{r}) h_l(\mathbf{r}) d^3\mathbf{r}.$$

Using the orthogonal condition (12.8), we get

$$\int_V m(\mathbf{r}) h_l(\mathbf{r}) d^3\mathbf{r} = \sum_k a_k \delta_{kl} = a_l.$$

**Exercise 12.3** For an arbitrary corner of the rectangular box  $(x_l, y_m, z_n)$ , (B12.7) becomes

$$m(x_l, y_m, z_n) = \sum_{i,j,k=1}^2 m(x_l, y_m, z_n) \left(1 - \frac{|x_l - x_i|}{x_2 - x_1}\right) \left(1 - \frac{|y_m - y_j|}{y_2 - y_1}\right) \left(1 - \frac{|z_n - z_k|}{z_2 - z_1}\right). \quad (12.10)$$

Whenever indices in the numerators are unequal, both numerator and denominator are equal to the length of the box. Therefore, the only nonzero term in this sum occurs when  $i = l, j = m, k = n$ , so that

$$m(x_l, y_m, z_n) = m(x_l, y_m, z_n) \times 1 \times 1 \times 1 = m(x_l, y_m, z_n).$$

Therefore, the interpolated value of any corner equals the assigned value of that corner.

**Exercise 12.4** The penalty function is (B12.10):

$$E = \sum_{i=1}^N \sum_{j \in \mathcal{N}_i} \frac{(L_{ij} - l_{ij})^2}{l_{ij}^2},$$

where  $L_{ij} = \sqrt{(x_i - x_j)^2 + (y_i - y_j)^2 + (z_i - z_j)^2}$  and the  $l_{ij}$  are given.  $E$  sums over all natural neighbours of node  $i$ ; on the other hand, node  $i$  is the natural neighbour for any  $j \in \mathcal{N}_i$ . Therefore, every node pair  $(i, j)$  appears twice in the sum:

$$\begin{aligned} \frac{\partial E}{\partial x_k} &= 2 \frac{\partial}{\partial x_k} \sum_{j \in \mathcal{N}_k} \frac{(L_{kj} - l_{kj})^2}{l_{kj}^2} = 4 \sum_{j \in \mathcal{N}_k} \frac{L_{kj} - l_{kj}}{l_{kj}^2} \frac{\partial L_{kj}}{\partial x_k} \\ &= 4 \sum_{j \in \mathcal{N}_k} \frac{L_{kj} - l_{kj}}{l_{kj}^2} \times \frac{1}{2} \frac{2(x_k - x_j)}{L_{kj}} = \sum_{j \in \mathcal{N}_k} 4 \left(1 - \frac{l_{kj}}{L_{kj}}\right) \frac{x_k - x_j}{l_{kj}^2}. \end{aligned}$$

**Exercise 12.5** The excess topography is given by

$$t_e(\theta) = -\epsilon \frac{2}{3} P_2^0(\cos \theta). \quad (12.11)$$

We recognize

$$P_2^0(\cos \theta) = \left(\frac{5}{4\pi}\right)^{-\frac{1}{2}} X_2^0(\theta).$$

Since  $t_e(\theta)$  has only one nonzero harmonic term, with  $P_2^0(\cos \theta)$ , the only nonzero coefficient is  $a_{20}$ . We use the expression in Section B12.4 and the orthogonality of  $X_\ell^m$ :

$$a_{20} = -2\pi \frac{2}{3} \epsilon \left( \frac{5}{4\pi} \right)^{-\frac{1}{2}} \int_0^\pi X_2^0 X_2^0 \sin \theta d\theta = -\frac{2}{3} \epsilon \left( \frac{5}{4\pi} \right)^{-\frac{1}{2}}.$$

# 13

## Common corrections

**Exercise 13.1** If  $p(\Delta)$  is the slowness of the wave arriving at distance  $\Delta$ :

$$\tau(\Delta) = T(\Delta) - p(\Delta)\Delta, \quad (13.1)$$

with

$$p(\Delta) = \frac{dT(\Delta)}{d\Delta}. \quad (13.2)$$

Differentiate (13.1) w.r.t.  $\Delta$ :

$$\frac{d\tau}{d\Delta} = \frac{dT}{d\Delta} - p(\Delta) - \frac{dp}{d\Delta}\Delta = -\frac{dp}{d\Delta}\Delta,$$

where the last step uses (13.2). Then

$$\frac{d\tau}{dp} = \frac{d\tau}{d\Delta} \frac{d\Delta}{dp} = -\frac{dp}{d\Delta}\Delta \cdot \frac{d\Delta}{dp} = -\Delta.$$

Since  $\Delta > 0$ , the intercept time  $\tau$  is a monotonically decreasing function of  $p$ .

**Exercise 13.2** In local problems, we use the Cartesian coordinates. Then  $p = \sin i/c$  and the epicentral distance is measured by  $X$  (dimension of length). In Figure B13.5, sea level  $r = a$  corresponds to  $z = 0$  in the Cartesian coordinates, and  $r = a + h$  corresponds to  $z = h$ . Similar to the spherical case, we have

$$\delta t_{(p=\text{constant})} = 2 \int_0^h \frac{dz}{c \cos i},$$

$$\delta X = 2 \int_0^h \tan i \, dz = 2 \int_0^h \frac{\sin i}{\cos i} \, dz.$$

Then

$$\delta\tau = \delta t_{(\Delta=\text{constant})} = \delta t_{(p=\text{constant})} - p\delta X = 2 \int_0^h \left( \frac{1}{c \cos i} - \frac{p \sin i}{\cos i} \right) dz.$$

Using  $p = \sin i/c$ , we get

$$\delta\tau = 2 \int_0^h \left( \frac{1}{c} - \frac{\sin^2 i}{c} \right) \frac{dz}{\cos i} = 2 \int_0^h \frac{\cos i}{c} dz = 2 \int_0^h \frac{1}{c} \sqrt{1 - p^2 c^2} dz,$$

**Exercise 13.3** In a spherical earth,  $p = r \sin i/c$ ,  $\cos i = \sqrt{1 - \sin^2 i} = \sqrt{1 - p^2 c^2/r^2}$ . Then (B13.5) can be written as

$$\tau = 2 \int_a^{a+h} \frac{\cos i}{c} dr = \int_a^{a+h} \frac{\cos i_1}{c_1} dr + \int_a^{a+h} \frac{\cos i_2}{c_2} dr,$$

where the first integral is for the incoming wave, and the second integral is for the reflected wave. Straight rays imply that the velocities  $c_1, c_2$  and the incidence angles  $i_1, i_2$  are constants, so

$$\tau = \frac{\cos i_1}{c_1} \int_a^{a+h} dr + \frac{\cos i_2}{c_2} \int_a^{a+h} dr = h \left( \frac{\cos i_1}{c_1} + \frac{\cos i_2}{c_2} \right). \quad (13.3)$$

This topographic correction conforms to (B13.3). Because a surface reflection is always an underside reflection, there is only a positive sign in (13.3), though  $h$  can be either positive or negative.

# 14

## Linear inversion

**Exercise 14.1** With univariant data ( $\sigma_i = 1$ ), the expression for  $\chi^2$  is

$$\chi^2(\mathbf{m}) = \sum_{i=1}^N \left( \sum_{j=1}^M A_{ij} m_j - d_i \right)^2. \quad (14.1)$$

To minimize (14.1), all derivatives with respect to  $m_k$  ( $k = 1, \dots, M$ ) should be zero:

$$\begin{aligned} \frac{\partial \chi^2}{\partial m_k} &= \frac{\partial}{\partial m_k} \sum_{i=1}^N \left( \sum_{j=1}^M A_{ij} m_j - d_i \right) \left( \sum_{l=1}^M A_{il} m_l - d_i \right) \\ &= \sum_{i=1}^N 2 \left( \sum_{j=1}^M A_{ij} m_j - d_i \right) A_{ik} \\ &= 2 \sum_{i=1}^N \sum_{j=1}^M A_{ki}^T A_{ij} m_j - 2 \sum_{i=1}^N A_{ki}^T d_i = 0. \end{aligned}$$

The matrix form of the last equation is (after dividing by 2):

$$\mathbf{A}^T \mathbf{A} \mathbf{m} - \mathbf{A}^T \mathbf{d} = 0.$$

**Exercise 14.2** Because no inverse for  $\mathbf{A}^T$  exists, the linear equations  $\mathbf{A}^T \mathbf{x} = 0$  have non-zero solutions.

**Exercise 14.3** From (B14.12):

$$\mathbf{V}^T \mathbf{A}^T = \mathbf{\Lambda} \mathbf{U}^T.$$

Multiply on the right by  $U$ :

$$\mathbf{V}^T \mathbf{A}^T \mathbf{U} = \mathbf{\Lambda} \mathbf{U}^T \mathbf{U}.$$

Apply (B14.11) and the orthonormality of  $\mathbf{V}$ :

$$\mathbf{V}^T \mathbf{V} \mathbf{\Lambda} = \mathbf{\Lambda} = \mathbf{\Lambda} \mathbf{U}^T \mathbf{U},$$

from which it immediately follows that the  $\mathbf{u}_i$  are orthonormal if  $\lambda_i \neq 0$ . For zero eigenvalues the normalization of  $\mathbf{u}_i$  is arbitrary. We can set the length to 1 without affecting (B14.11) in any way.

**Exercise 14.4** Taking the transpose of (B14.14):

$$\mathbf{A}^T = \mathbf{V}_K \mathbf{\Lambda}_K \mathbf{U}_K^T,$$

and inserting this into (B14.7):

$$\begin{aligned} \hat{\mathbf{m}} &= \mathbf{V}_K \mathbf{\Lambda}_K^{-2} \mathbf{V}_K^T \mathbf{A}^T \mathbf{d} = \mathbf{V}_K \mathbf{\Lambda}_K^{-2} \mathbf{V}_K^T \mathbf{V}_K \mathbf{\Lambda}_K \mathbf{U}_K^T \mathbf{d} \\ &= \mathbf{V}_K \mathbf{\Lambda}_K^{-2} \mathbf{\Lambda}_K \mathbf{U}_K^T \mathbf{d} = \mathbf{V}_K \mathbf{\Lambda}_K^{-1} \mathbf{U}_K^T \mathbf{d}. \end{aligned}$$

**Exercise 14.5** The normal equations for (B14.15) are found by multiplying left and right with the transpose of the matrix:

$$\begin{pmatrix} \mathbf{A}^T & \epsilon_n \mathbf{I} \end{pmatrix} \begin{pmatrix} \mathbf{A} \\ \epsilon_n \mathbf{I} \end{pmatrix} \mathbf{m} = \begin{pmatrix} \mathbf{A}^T & \epsilon_n \mathbf{I} \end{pmatrix} \begin{pmatrix} \mathbf{d} \\ \mathbf{0} \end{pmatrix}$$

Multiplying the matrices:

$$(\mathbf{A}^T \mathbf{A} + \epsilon_n^2 \mathbf{I}) \mathbf{m} = \mathbf{A}^T \mathbf{d}.$$

**Exercise 14.6** In the L-curve (Fig. B14.2), the rightmost point has the smallest  $\chi^2$  and the largest  $|\mathbf{m}|$ , so this is where  $\epsilon_n = 0$ . The intercept with the vertical axis has the largest  $\chi^2$  and the smallest  $|\mathbf{m}|$ , so this is where  $\epsilon_n \rightarrow \infty$ .

# 15

## Resolution and error analysis

**Exercise 15.1** Because such an arbitrarily scaled model does not satisfy the linear system

$$Am = d.$$

The fact that we increase the estimate of the model variance does not make up for the fact that we do not guarantee that the scaled model satisfies the data at an acceptable  $\chi^2$  level.

# 16

## Anisotropy

**Exercise 16.1** Expression (B16.1) gives the Voight matrix for isotropic solids:

$$\begin{pmatrix} \lambda + 2\mu & \lambda & \lambda & 0 & 0 & 0 \\ \lambda & \lambda + 2\mu & \lambda & 0 & 0 & 0 \\ \lambda & \lambda & \lambda + 2\mu & 0 & 0 & 0 \\ 0 & 0 & 0 & \mu & 0 & 0 \\ 0 & 0 & 0 & 0 & \mu & 0 \\ 0 & 0 & 0 & 0 & 0 & \mu \end{pmatrix}.$$

The first three rows/columns involve the combinations  $xx$ ,  $yy$  and  $zz$ . Exchange of  $x$  and  $y$ , for example, leaves the diagonal and off-diagonal elements the same, and so for other exchanges. For the pairs  $yz, xz$  and  $xy$  in columns 4,5,6, exchange results in exchange of diagonal elements that are all equal to  $\mu$ , so there is no change in the Voight matrix.

**Exercise 16.2** For hexagonal symmetry we have:

$$\begin{pmatrix} A & A - 2N & F & 0 & 0 & 0 \\ A - 2N & A & F & 0 & 0 & 0 \\ F & F & C & 0 & 0 & 0 \\ 0 & 0 & 0 & L & 0 & 0 \\ 0 & 0 & 0 & 0 & L & 0 \\ 0 & 0 & 0 & 0 & 0 & N \end{pmatrix}.$$

As long as we leave the  $z$ -axis untouched, the third and sixth row and column do not change. The symmetry in the other rows/columns is as in the previous exercise, so again the matrix is invariant.